AD_____

Award Number:
W81XWH-11-2-0065

TITLE:
Development of Pantothenate Analogs That Can Treat Combat-Related Infections

PRINCIPAL INVESTIGATOR:
Hee-Won Park, PhD

CONTRACTING ORGANIZATION:
Tulane University School of Medicine
New Orleans, LA 70112

REPORT DATE: APRIL 2014

TYPE OF REPORT: FINAL

PREPARED FOR: U.S. Army Medical Research and Materiel Command
Fort Detrick, Maryland 21702-5012

REPORT DOCUMENTATION PAGE

Form Approved
OMB No. 0704-0188

1. REPORT DATE	2. REPORT TYPE	3. DATES COVERED
April 2014	Final	1 Jan 2011 - 31 Dec 2013

4. TITLE AND SUBTITLE
Development of Pantothenate Analogs That Can Treat Combat-Related Infections

5a. CONTRACT NUMBER

5b. GRANT NUMBER
W81XWH-11-2-0065

5c. PROGRAM ELEMENT NUMBER

6. AUTHOR(S)
Hee-Won Park

E-Mail: hpark1@tulane.edu

5d. PROJECT NUMBER

5e. TASK NUMBER

5f. WORK UNIT NUMBER

7. PERFORMING ORGANIZATION NAME(S) AND ADDRESS(ES)
Tulane University School of Medicine

New Orleans, LA 70112

8. PERFORMING ORGANIZATION REPORT NUMBER

9. SPONSORING / MONITORING AGENCY NAME(S) AND ADDRESS(ES)
U.S. Army Medical Research and Materiel Command
Fort Detrick, Maryland 21702-5012

10. SPONSOR/MONITOR'S ACRONYM(S)

11. SPONSOR/MONITOR'S REPORT NUMBER(S)

12. DISTRIBUTION / AVAILABILITY STATEMENT
Approved for Public Release; Distribution Unlimited

13. SUPPLEMENTARY NOTES

14. ABSTRACT

Increasing reports of antibiotic resistance involving *S. aureus* and *K. pneumoniae* and the resulting high mortality rates in the battlefields have emphasized a critical need for the development of antimicrobial compounds with novel modes of action. Fatty acids are known to serve many critical roles in the cell, including energy storage, integrity and dynamics of biological membranes, cellular metabolism, and cellular signaling, and interference with fatty acid metabolism has been proved to be an effective strategy for inhibition of bacterial growth. N-substituted pantothenate analogs have been developed and shown to inhibit the growth of *S. aureus* and *E. coli* (and probably also *K. pneumoniae*) but have not been tested in preclinical and clinical set-ups, primarily because of their possible interference with human cells. We propose to elucidate differences in the architecture of the compound-pantothenate kinase-binding site between humans and bacteria using x-ray crystallographic techniques and exploit these differences to develop new compounds specific for the drug-resistant bacterial strains. These new compounds will have the potential to control infections caused by *S. aureus* and *K. pneumoniae*, thus improving the survival rate of military personnel wounded in combat. Candidate compounds identified in this study should first be tested in animal models to determine their response to the treatment and subsequently in clinical trials to test the efficacy of this novel approach in humans. Our efficient procedure of the iteration of the computer prediction and experimental verifications with the sufficient feedback will enable us to identify novel drug candidates, which are characterized by fewer side-effects, less likelihood of drug resistance, and will be available to public at costs substantially below industry average.

15. SUBJECT TERMS
Antibiotics, drug development, multi-drug resistant bacterial strains, crystallography, coenzyme A biosynthesis, pantothenate (vitamin B5) kinase

16. SECURITY CLASSIFICATION OF:			17. LIMITATION OF ABSTRACT	18. NUMBER OF PAGES	19a. NAME OF RESPONSIBLE PERSON
a. REPORT	b. ABSTRACT	c. THIS PAGE			19b. TELEPHONE NUMBER *(include area code)*
U	U	U	UU	37	USAMRMC

Table of Contents

Introduction

A goal of the studies is to develop antimicrobial compounds with novel modes of action to treat the battlefield infections from *Staphylococcus aureus, Klebsiella pneumoniae* and extended-spectrum beta-lactamase enterobacteriaceae including *E. coli*. N-substituted pantothenate analogs have been developed and shown to inhibit the growth of *S. aureus* and *E. coli* (and probably also *K. pneumoniae*) but have not been tested in preclinical and clinical set-ups, primarily because of their possible interference with human cells. We propose to elucidate differences in the architecture of the compound-pantothenate kinase binding site between humans and bacteria using x-ray crystallographic techniques and exploit these differences to develop new compounds specific for the drug-resistant bacterial strains.

Body

The following research accomplishments are described according to each task outlined in the approved Statement of Work.

Task 1. Structural studies of the pantothenate binding site of PanKs from human and three bacteria strains that cause high mortality (*S. aureus*, *K. pneumoniae,* and *E. coli*) and the interactions of the binding site with known pantothenate analogs (months 1-24)

1. Crystallographic refinement of the co-crystal structure of *S. aureus* PanK (SaPanK) complexed with N5-Pan (months 1-3)

We solved the structure of the SaPanK•N5-Pan complex by the molecular replacement method with a search model of the ATP-bound SaPanK structure (PDB code 2EWS), followed by several rounds of model building, refinement and validation. The co-crystallization of SaPanK with N5-Pan was carried out in the presence of ATP molecule, but the resulting N5-Pan was in phosphorylated form and ADP, instead of ATP, was found at the binding site (The left panel in Fig. 1)(Supporting data, p26), suggesting that ATP was converted to ADP with the phosphorylation of N5-Pan (Pho-N5-Pan). This finding is consistent with the fact that N5-Pan is a substrate of SaPanK. The hydrophobic portions of multiple residues (Leu171, Thr172, Glu202, Val236 and Tyr240) form a non-polar tunnel that accommodates the pentyl tail of Pho-N5-Pan (The right panel in Fig. 1)(Supporting data, p26).

Figure 1. SaPanK structure. *Left,* phosphorylation of N5-Pan in the presence of ATP. Dotted-circle indicates the phosphate group of p-N5-Pan. *Right,* p-N5-Pan interacting residues at the binding site of SaPanK. P-N5-Pan (yellow) and the interacting residues are shown in ball-and stick representation. Dotted-line indicates polar interactions.

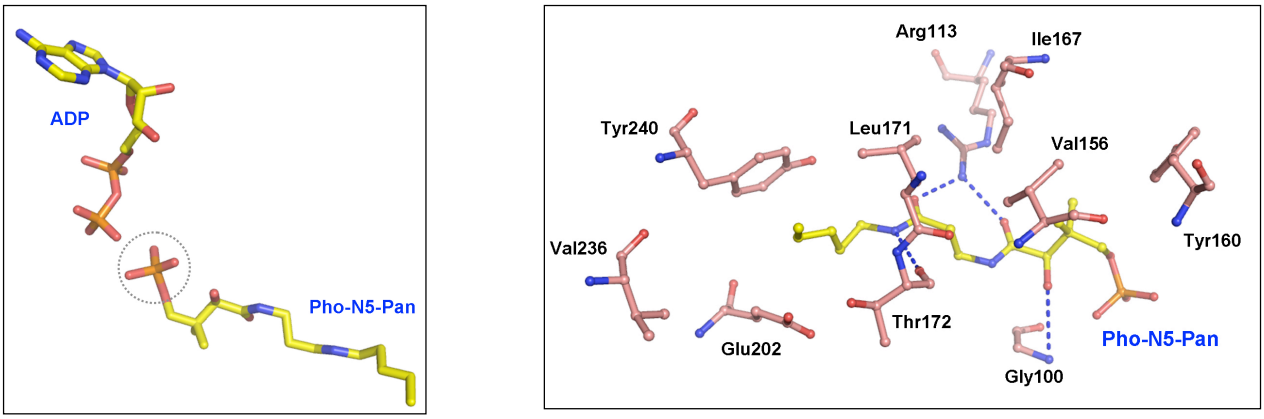

2. Crystal growth and structure determination of *S. aureus* PanK complexed with N7-Pan (month 3-6)

The gene of SaPanK was from its genomic DNA library and was subcloned into a bacterial expression vector pET28a. The resulting plasmid contained the NH_2-terminal hexaHis tag fused to the PanK protein. We used *E. coli* BL21(DE3) (Stratagene) for protein expression and for protein purification nickel-nitrilotriacetic acid affinity and Superdex 200 (GE Healthcare) gel-filtration columns. N7-Pan was co-crystallized with SaPanK in the presence of ATP. Similar to the N5-Pan structure, ATP

and N7-Pan were converted to ADP and the phosphorylated N7-Pan (Pho-N7-Pan), respectively. The mode of binding between Pho-N5-Pan and Pho-N7-Pan in both crystal structures of SaPanK was identical (Fig. 2)(Supporting data, p27), which is well reflected in the same orientation of the surrounding residues. N7-Pan analog has two more methyl groups at the N-substituted tail than that of N5-Pan. Electron density corresponding to these two methyl groups of N7-Pan is invisible and thus disordered in the structure due to no contact with SaPanK residues. Therefore, the extra two methyl groups of N7-Pan may not be needed for the binding to SaPanK.

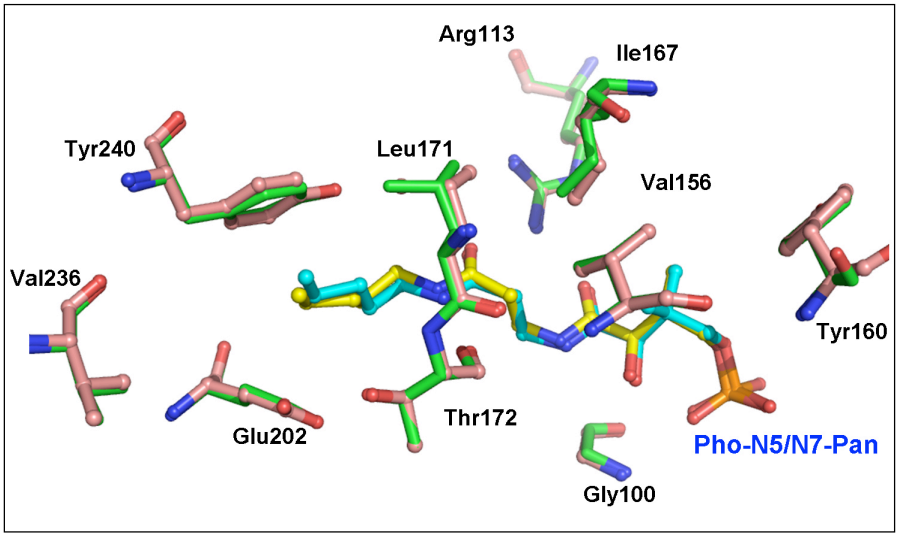

Figure 2. Superposition of Pho-N5-Pan and Pho-N7-Pan at the binding site. Carbon atoms of the two analogs are in yellow and cyan, respectively. The binding site residues for Pho-N5-Pan and Pho-N7-Pan are in skin and green.

3. Protein expression and purification, crystal growth and structure determination of *K. pneumoniae* PanK in complex with Pan analogs (months 6-24)

The gene of *K. pneumoniae* (KpPanK) was chemically synthesized by GenScript. Subcloning, expression and purification are the same as SaPanK (see the section 2 of Task 1). We solved the structure of KpPanK complexed with N7-Pan. The N7-Pan binding site has polar properties different from that of hPanK3, particularly those surrounding the N7Pan hydrophobic tail region. The N7-Pan aliphatic tail in hPanK3 is found within a relatively polar environment, surrounded by N299, S303 and R306 (The left panel in Fig. 3)(Supporting data, p28). In contrast, the aliphatic tail of N7-Pan in KpPanK is bent towards a hydrophobic pocket containing multiple phenyl-containing residues (The right panel in Fig. 3)(Supporting data, p28). This difference will be the basis to develop new compounds specific for KpPanK with minimal affinity to hPanK3.

Figure 3. The N7-binding sites of PanKs. *Left,* the N7 moiety (green) is bound by polar residues, W341, R306 and S303 and N299 of hPanK3. *Right,* the N7-moiety (green) is bound by hydrophobic residues, Y258, F259, F247, F244 and Y240.

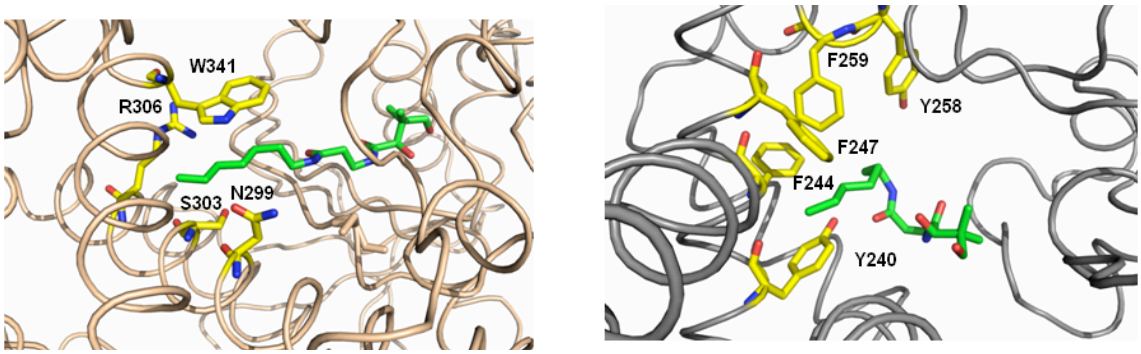

4. Protein expression and purification, crystal growth and structure determination of *E. coli* PanK in complex with Pan analogs (months 3-12)

The gene of *E. coli* pantothenate kinase (EcPanK) was chemically synthesized by GenScript. Subcloning, expression and purification are the same as SaPanK (see the section 2 of Task 1). We co-

crystallized EcPanK in complex with N5-Pan and solved the structure. Similar to KpPanK, the hydrophobic tail of N5-Pan in the EcPanK structure was bent to form a U-shape (Fig. 4)(Supporting data, p29). The conformational differences of the analogs between EcPanK and hPanK3 as well as the amino acid differences lining the substituents of N-substituted Pan analog will be the basis to develop new compounds specifically interfering with the activity of EcPanK.

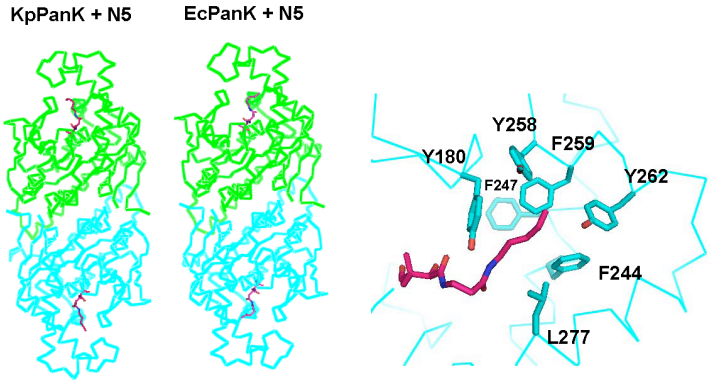

Figure 4. Co-crystal structures of KpPanK and EcPanK with N5-Pan. *Left,* both the structures of KpPanK and EcPanK are dimeric (green and cyan). N5-Pan is bound to only one molecule. *Right,* a zoomed-in view of the N5-Pan binding site of EcPanK shows the bending of N5, similar to that of KpPanK. Non-polar aromatic residues of EcPanK interacting with the pentyl moiety of N5-Pan are labeled.

5. Protein expression and purification, crystal growth and structure determination of human PanK1, PanK2 and PanK3 in complex with Pan analogs (months 6-24)

The gene of human pantothenate kinase isoform 3 (hPanK3) was from the Mammalian Gene Collection and was subcloned into a bacterial expression vector pET28a. The resulting plasmid contained the NH_2-terminal hexaHis tag fused to the PanK protein. We used *E. coli* BL21(DE3) (Stratagene) for protein expression and for protein purification nickel-nitrilotriacetic acid affinity and Superdex 200 (GE Healthcare) gel-filtration columns. We co-crystallized hPanK3 with N7-Pan analogs and solved the structure by molecular replacement. Detailed description for molecular replacement structure determination was given in the first section of Task 1. The structure shows that N7-Pan was bound to hPanK3, similar to SaPanK. The bound analog interacts with the beta-barrel from one molecule of dimeric hPanK3 and also with a loop region of the other molecule (Fig. 5)(Supporting data, p30). Unlike in SaPanK, however, N7-Pan in hPanK3 was not phosphorylated. This finding suggests possible differences between SaPanK and hPanK in their enzymatic activities toward N7-Pan.

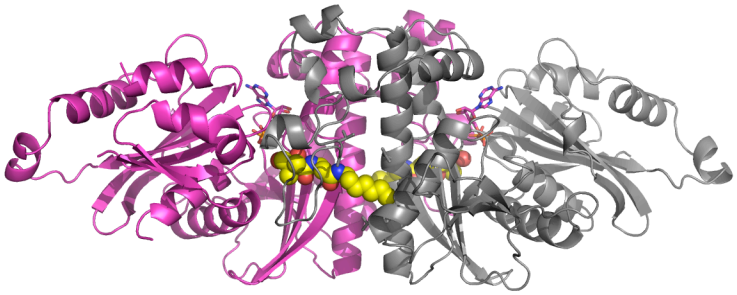

Figure 5. Overall structure of dimeric Human PanK3 complexed with N7-Pan. The bound Pan-analog was presented in a space-filling model.

Figure 6. *Left*, sructural superimposition of N7-Pan bound SaPanK (cyan) and hPanK3 (magenta). *Middle,* zoomed view of overlapped N7-Pan analogs from SaPanK (cyan) and hPanK3 (magenta). *Right,* difference in the interaction mode of N7-Pan analogs observed between SaPanK (cyan) and hPanK3 (magenta).

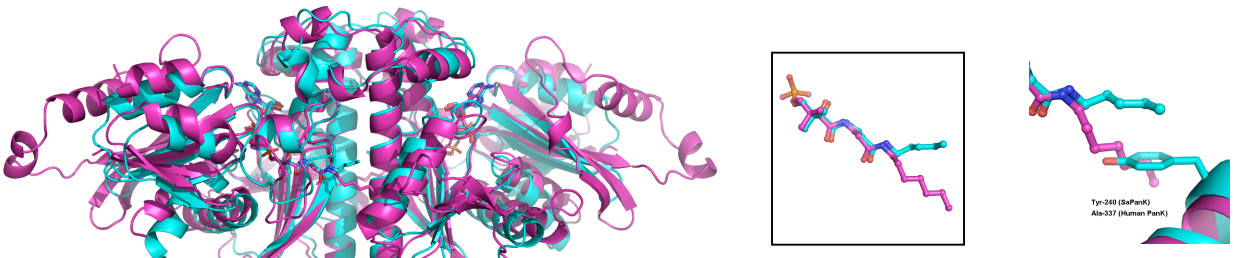

To analyze the interaction mode of SaPanK and hPanK with the Pan analogs, we superimposed the structures of N7-Pan bound SaPanK and hPanK3 (The left and middle panels in Fig. 6)(Supporting data,

p31). The pantothenate moieties of the N7-Pan analogs were well overlapped while the hydrophobic tail regions were poorly superimposed. This conformational difference between SaPanK and hPanK3 could be explained by the difference of resides lining the hydrophobic tail binding pocket. Among these residues, we specially paid attention to Tyr240 of SaPanK, which is replaced by Ala337 of hPanK3 (The right panel in Fig. 6)(Supporting data, p31). Structurally, the bulky Tyr240 of SaPanK was oriented toward the N7 tail, bending the N7 tail to avoid a steric hindrance and exposing the last two methyl groups of the N7 tail to solvent. In contrast, the short side chain of Ala-337 of hPanK3 accommodated the N7 tail without problem.

Task 2. Structure-based/virtual design of specific high-affinity analogs and their characterization using *in vitro* biochemical assays and *in vivo* bacterial colony and human cell cytotoxicity assays (months 6-36). The following five sub-tasks will be repeated until we identify the experimentally verified candidate compounds possessing low human cell cytotoxicity.

1. Computational prediction of a drug-like chemical series against bacterial PanKs (months 3-12)

   Based on the differences of the N7-Pan heptyl group binding sites between bacterial PanKs and hPanK3, we initially synthesized two new compounds MT-0183 and MT-0190 (Fig. 7)(Supporting data, p32) and eleven additional compounds MT-0348, MT-0349, MT-0350, MT-0351, MT-0352, MT-0353, MT-0354, MT-0355, MT-0356, MT-0357 and MT-0358 (Fig. 7)(Supporting data, p32).

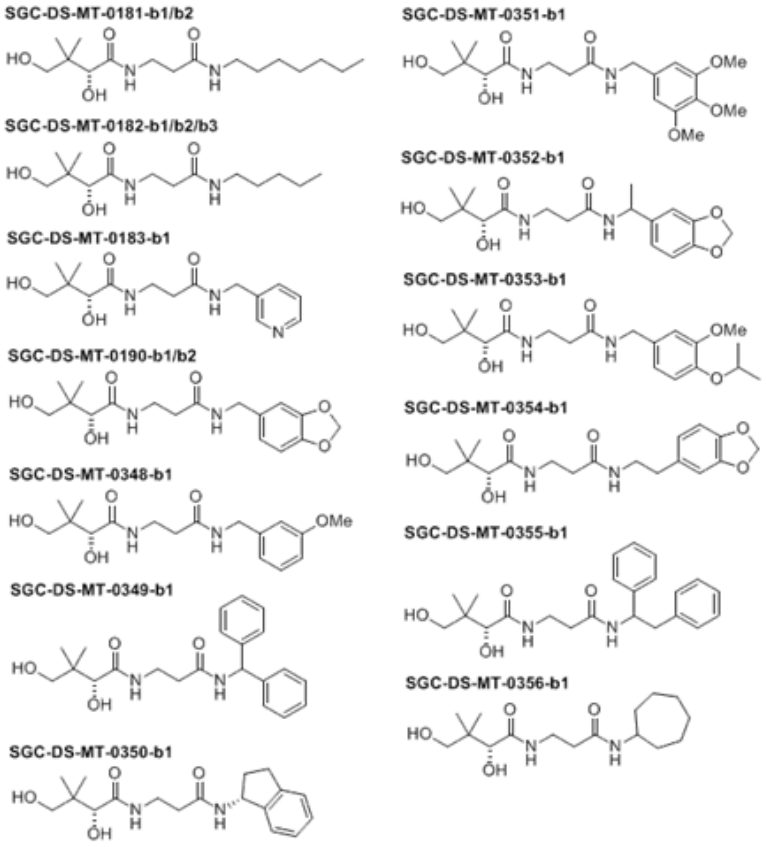

Figure 7. A new set of Pan analogs including MT-0183 and MT-0190 as well as N5-Pan (MT-182) and N7-Pan (MT-181)

2. Investigate inhibitory effects of the candidate compounds using the standard pantothenate kinase assay (months 6-36)

   To confirm that all recombinant PanK proteins expressed in E. coli are fully active, the enzymatic activities were measured using the PK/LDH coupled assay and relatively compared to that of SaPanK. All the tested bacterial PanKs were fully active (Fig. 8)(Supporting data, p33). The activity of hPanK3 was relatively low, probably due to the partial occupancy of the acetyl-CoA inhibitor co-purified from E. coli cells. These results suggest that the recombinant PanK proteins are fully active and we can use the PK/LDH coupled assay for investigating inhibitory effects of the Pan analogs.

In the 4th quarter of 2013, we measured the activities of SaPanK using the PK/LDH coupled assay. Compared to pantothenate, three of four analogs (N5-Pan, N7-Pan and MT-0190) were weak substrates

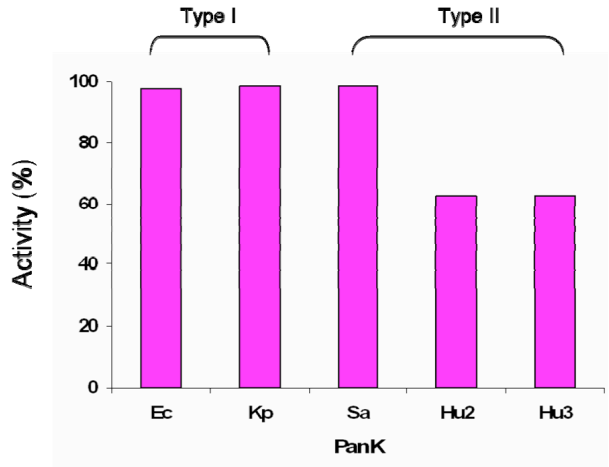

Figure 8. Relative activities of recombinant pantothenate kinases . The activities are normalized to that of SaPanK. Ec: EcPank, Kp: KpPanK, Sa: SaPanK, Hu2: hPanK2, Hu3: hPanK3.

for SaPanK. Especially SaPanK showed almost no activity with MT-0190. Consistent with this finding, these analogs were found to inhibit SaPanK effectively (IC_{50} values were 5.3 uM, 2.8 uM and 0.7 uM).

3. Determine the minimum inhibitory concentrations of the candidate compounds using a broth dilution method (months 9-36)

In the 4th quarter of 2011, we measured the MICs (Minimum Inhibitory Concentration) of N5-Pan and N7-Pan against *Enterococcus faecalis* ATCC 29212 and *S. aureus* ATCC 29213 by using a broth microdilution assay. The results of the MIC assays are as follows: the MIC for *Enterococcus faecalis* was determined as 156 ug/ml for N5-Pan and 29 ug/ml for N7-Pan, respectively. In the case of *S. aureus*, however, its MIC values to both Pan analogs could not be determined, because cells did not grow even at the given minimal concentration (9.8 ug/ml) of both Pan analogs.

In the 1st quarter of 2012, we determined the MICs of MT-0183 and MT-0190 against *S. aureus* ATCC 29213, *K. pneumoniae* ATCC 10031 and *E. coli* ATCC 25922 by using broth microdilution assay. MT-0190 showed the MIC of 250 µg/ml for *S. aureus* and higher MICs (>2.0 mg/ml) for *E. coli* and *P. pneumoniae*. MT-0183 showed the MIC of 1 mg/ml for *P. pneumoniae* and higher MICs (>2.0 mg/ml) for *E. coli* and *S. aureus*. We also solved the co-crystal structure of SaPanK with MT-0190.

In the 1st quarter of 2013, we assessed the bacterial-killing capability of the 11 compounds against *S. aureus* ATCC 29213, *K. pneumoniae* ATCC 10031 and *E. coli* ATCC 25922 by using agar diffusion assay. The compounds MT-0348 and MT-0356 effectively inhibited the growth of *S. aureus* but the same compounds were ineffective against *K. pneumoniae* and *E. coli*.

In the 2nd quarter of 2013, our MIC assay showed that HOPA inhibited the growth of bacterial cells at the concentration of 100 ug/ml (Fig. 9)(Supporting data, p34).

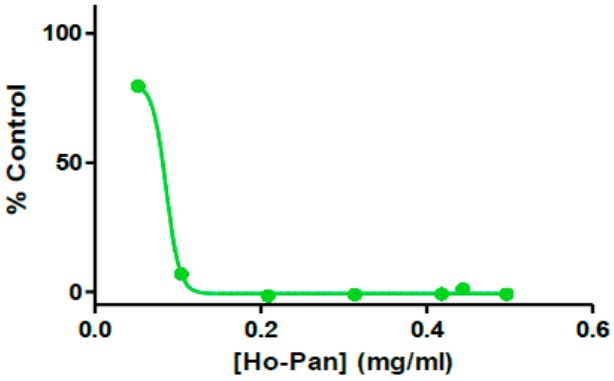

Figure 9. MIC assay of HOPA against S. aureus. Bacteria (5 x 1010 cfu/ml) were grown for one day with increasing conc. of the compound. Data is shown as percent OD600 of control.

4. Crystallographic verification of binding for the most promising candidates (months 12-36)

To achieve optimal lead compounds from MT-0190, we solved the co-crystal structure of SaPanK with MT-0190. The hydrophobic portions of several residues (Leu171, Thr172, Glu202, Val236 and Tyr240) form a non-polar pocket for the aromatic moiety of MT-0190 (Fig. 10)(Supporting data, p35). We noticed that the same residues are involved in forming the binding pocket of SaPanK for N7-Pan (Fig. 1 & 2)(Supporting data, p26&27). Importantly, the aromatic moiety of MT-0190 is inserted in between the side chains of Glu202 and Tyr240 as Glu202 is stabilized by Thr172 via a side chain hydrogen bond (Fig. 10)(Supporting data, p35). More importantly, there is a space between the aromatic moiety of MT-0190 and Val236, which can direct additional structural modifications of MT-0190 specific for SaPanK.

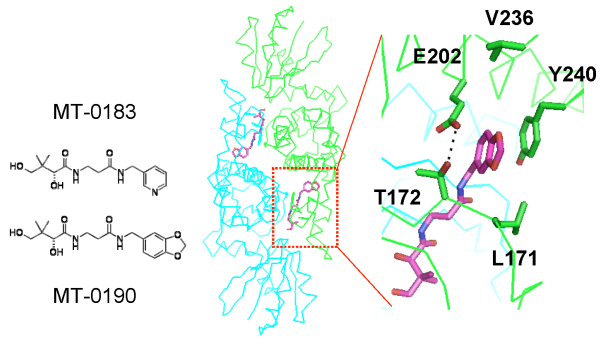

Figure 10. The MT-0190 binding site of SaPanK. *Left,* MT-183 and MT-190 Pan analogs. *Middle,* MT-0190 (magenta, stick) is bound to both the molecules of SaPank dimer (green and cyan). *Right,* the aromatic moiety of MT-0190 (magenta, carbon) interacts with hydrophobic portions of several residues, L171, T172, E202, V236 and Y240. Dotted line indicates a hydrogen bond between T172 and E202.

Similar to MT-0190, we co-crystallized KpPanK with MT-0183 and solved the structure of the KpPanK•MT-0183 complex. We solved the structure of the KpPanK in complex with N5-Pan at 2.1Å resolution. In the structure, the nitrogen-substituted benzyl moiety of MT-0183 is surrounded by multiple non-polar residues providing hydrophobic contacts (Fig. 11) (Supporting data, p36) (Appendix, Li at al., 2013). A surprising observation is that the benzyl moiety can be bound at the active site in two alternative conformations (Fig. 11) (Supporting data, p36) (Appendix, Li at al., 2013). This finding suggests that a branched compound (e.g., a substituent with two benzyl moieties) may improve binding potency toward KpPanK.

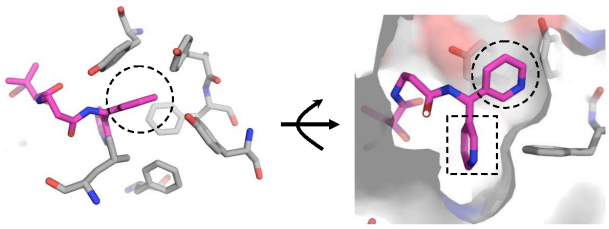

Figure 11. The MT-183 binding pocket of KpPanK. *Left,* a view showing the benzyl moiety interactions with hydrophobic residues of KpPanK (Y180, F244, Y258, F259 and Y262). Dotted circle indicates the benzyl moiety. *Right,* a view with a horizontal rotation of 90 degrees from the left panel. Dotted circle indicates the same benzyl moiety as in the left panel whereas dotted rectangle shows an alternative binding conformation of the benzyl moiety supported by electron density (data not shown).

In the 3rd quarter of 2013, we solved the structures of PanK from *K. pneumoniae* and *S. aureus* in complex with a newly synthesized pantothenate analog, N-[2-(1,3-benzodioxol-5-yl)ethyl] pantothenamide (N354-Pan, MT-0354 in Fig. 7)(Supproting data, p32). N354-Pan adapts an extened conformation, binding to the elongaged pocket of SaPanK (The right panel in Fig. 12) (Supporting data, p37) whereas it is severely kinked in the middle and interacts with the narrow pocket of KpPanK (The left panel in Fig. 12) (Supporting data, p37) (Appendix, Hughes et al., 2014). This finding strongly suggests considering the conformational flexibility of pantothenate analogs as well as their binding pockets in new compound design.

5. Test the most promising candidates against proliferating human somatic cells (months 15-36)

In the 3rd quarter of 2011, we tested the compounds (N5-Pan, N7-Pan, MT-0183 and MT-0190 in Fig. 7) against proliferating human HepG2 liver cells for assessing their cytotoxicity potential. Only N7-Pan at concentration of 5 mM decreased the cell viability, indicating that none of compounds badly inhibit the growth of the human hepatocytes.

In the 1st quarter of 2013, we tested the 11 compounds against human HepG2 hepatocellular carcinoma cells for their cytotoxicity. Six compounds (MT-0348, 0350, 0351, 0352, 0356 and 0358 in Fig. 7) were not cytotoxic to HepG2 cells.

In the 2nd quarter of 2013, we tested HOPA that showed no cytotoxicity against HEK293 cells.

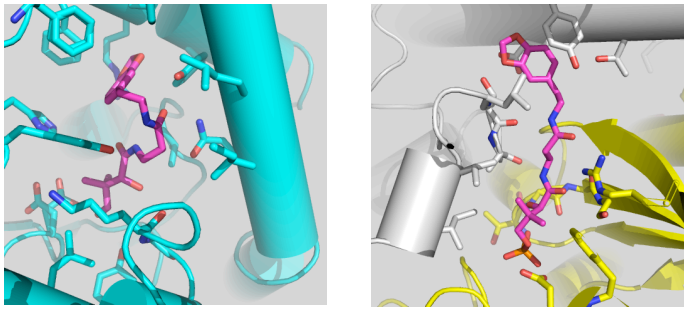

Figure 12. Interactions of N354-Pan with SaPanK and KpPanK. *Left,* the kinked conformation of N354-Pan (carbon, purple) interacting with multiple residues of KpPanK (carbon, cyan). *Right,* the extended conformation of N354 (carbon, purple) interacting with multiple residue of SaPanK (carbon, grey and yellow).

Key Research Accomplishments

- Structure determination of both N5- and N7-Pan bound to *S. aureus* PanK
- Structure determination of MT-0354 bound to *S. aureus* PanK
- Structure determination of N5-Pan bound to *K. pneumoniae* PanK
- Structure determination of MT-0354 bound to *K. pneumoniae* PanK
- Structure determination of MT-0183 bound to *K. pneumoniae* PanK
- Structure determination of N5-Pan bound *E. coli* PanK
- Structure determination of N7-Pan bound human PanK3
- Eight new compounds and HOPA showing no cytotoxicity to HepG2 liver cells
- Minimal inhibitory concentrations of MT-0190 and HOPA against *S. aureus* ~100 μg/ml.

Reportable Outcomes

Oral and invited presentations

1) An Oral presentation at 1st European Conference of Microbiology and Immunology in Budapest, Hungary between May 12-14, 2011, entitled "Crystal structure of *Staphylococcus aureus* pantothenate kinase in complex with a substrate analog N5-Pan."
2) An invited presentation at KonKuk University in Korea on Sep 14th, 2011, entitled "Targeted delivery of toxic vitamin B5 analogs into the bacterial cells".

Peer-reviewed publications

1) Li B, Tempel W, Smil D, Bolshan Y, Schapira M, Park HW. Crystal structures of *Klebsiella pneumoniae* pantothenate kinase in complex with N-substituted pantothenamides. PROTEINS. 81: 1466-1472, 2013.
2) Hughes SJ, Antoshchenko T, Kim KP, Smil D, Park HW. Structural characterization of a new N-substituted pantothenamide bound to pantothenate kinases from *Klebsiella pneumonia* and *Staphylococcus aureus.* PROTEINS. [Epub ahead of print], 2014.

Conclusion

These studies resulted in several new compounds (MT-0190, MT-0348 and MT-0356) that specifically inhibit the growth of *S. aureus* and one new compound (MT-0183) that specifically inhibit the growth of *K. pneumoniae*, as all of these new compounds have minimal effect on human cells. After potency optimization, these compounds can be the basis for testing in animal models in order to develop a novel class of antibiotics against the multidrug resistant strains of *S. aureus* and *K. pneumoniae* frequently found in battlefield wounds sustained in Iraq and Afghanistan.

References

1 Li, B. *et al.* Crystal structures of Klebsiella pneumoniae pantothenate kinase in complex with N-substituted pantothenamides. *Proteins* **81**, 1466-1472, doi:10.1002/prot.24290 (2013).

2 Hughes, S. J., Antoshchenko, T., Kim, K. P., Smil, D. & Park, H. W. Structural characterization of a new N-substituted pantothenamide bound to pantothenate kinases from Klebsiella pneumonia and Staphylococcus aureus. *Proteins*, doi:10.1002/prot.24524 (2014).

Appendices

Abstract for European Conference of Microbiology and Immunology

Crystal structure of *Staphylococcus aureus* pantothenate kinase in complex with a substrate analog N5-Pan.
Bum-Soo Hong[1] and Hee-Won Park[1,2]
[1]Structural Genomics Consortium, University of Toronto, 101 College Street, Toronto, Ontario, M5G 1L7, Canada.
[2]Department of Pharmacology and Toxicology, University of Toronto, 1 King's College Circle, Toronto, Ontario, M5S 1A8, Canada.

An objective of these studies is to advance targeted therapeutic intervention of staphylococcal infections by utilizing the pantothenate (vitamin B_5) substrate analogs of pantothenate kinase (PanK), the first step in the Coenzyme A biosynthetic pathway. The *S. aureus* PanK activity is inhibited by N-substituted pantothenate analogs, N-pentylpantothenamide (N5-Pan) and N-peptylpantothenamide (N7-Pan), and the growth rate of *S. aureus* cells is sensitive to N5-Pan and N7-Pan. The elucidation of differences between the human and bacterial enzymes, especially at the Pan analog binding site, will be of particular interest for the design of novel therapeutic compounds. The gene encoding *S. aureus* PanK was subcloned into a bacterial expression vector pET28a and PanK was expressed in *E. coli* BL21(DE3) cells. The protein was purified by a Ni-agarose affinity column and a S-200 Superdex gel filtration column on a FPLC system. Before crystallization, *S. aureus* PanK was mixed with ATP and N5-Pan. Crystals of the complex were obtained in 20% PEG5000 and 200mM KPO_4 and diffracted to 2.1 Å. The structure was determined by the molecular replacement method using the structure of *S. aureus* PanK excluding bound AMPPNP as a search model (PDB code 2EWS). The resulting structure of *S. aureus* PanK bound to N5-Pan identified residues involved in N5 recognition and provided the framework for understanding the detailed mechanism of the specificity of *S. aureus* PanK for N5-Pan. The N5-Pan-bound structure is being used for the design of novel therapeutic compounds against antibiotic-resistant stains of *Staphylococcus aureus*.

The two peer-reviewed articles of Reportable Outcomes are given in next pages.

1 Li, B. *et al.* Crystal structures of Klebsiella pneumoniae pantothenate kinase in complex with N-substituted pantothenamides. *Proteins* **81**, 1466-1472, doi:10.1002/prot.24290 (2013).

2 Hughes, S. J., Antoshchenko, T., Kim, K. P., Smil, D. & Park, H. W. Structural characterization of a new N-substituted pantothenamide bound to pantothenate kinases from Klebsiella pneumonia and Staphylococcus aureus. *Proteins*, doi:10.1002/prot.24524 (2014).

PROTEINS
STRUCTURE ■ FUNCTION ■ BIOINFORMATICS

STRUCTURE NOTE

Crystal structures of *Klebsiella pneumoniae* pantothenate kinase in complex with N-substituted pantothenamides

Buren Li,[1] Wolfram Tempel,[2] David Smil,[2] Yuri Bolshan,[2] Matthieu Schapira,[1,2] and Hee-Won Park[1,2]*

[1]Department of Pharmacology and Toxicology, University of Toronto, Toronto, Ontario M5S 1A8, Canada

[2]Structural Genomics Consortium, University of Toronto, Toronto, Ontario M5G 1L7, Canada

ABSTRACT

N-Substituted pantothenamides are derivatives of pantothenate, the precursor in the biosynthesis of the essential metabolic cofactor coenzyme A (CoA). These compounds are substrates of pantothenate kinase (PanK) in the first step of CoA biosynthesis and possess antimicrobial activity against various pathogenic bacteria. Here we solved the crystal structure of the *Klebsiella pneumoniae* PanK (KpPanK) in complex with N-pentylpantothenamide (N5-Pan) to understand the molecular basis of its antimicrobial activity. The structure reveals a polar pocket interacting with the pantothenate moiety of N5-Pan and an aromatic pocket loosely protecting the pentyl tail, suggesting that the introduction of an aromatic ring to a new pantothenamide may enhance the compound's affinity to KpPanK. To test this idea, we synthesized N-pyridin-3-ylmethylpantothenamide (Np-Pan) and solved its co-crystal structure with KpPanK. The structure reveals two alternat conformations of the aromatic ring of Np-Pan bound at the aromatic pocket, providing the basis for further improvement of pantothenamide binding to KpPanK.

Proteins 2013; 81:1466–1472

Key words: pantothenate kinase; vitamin B_5 analogs; CoA synthesis inhibitors; enzyme-substrate analog complex; X-ray crystallography.

Additional Supporting Information may be found in the online version of this article.

Abbreviations: ACP, acyl carrier protein; CoA, coenzyme A; EcPanK, *Escherichia coli* pantothenate kinase; KpPanK, *Klebsiella pneumoniae* pantothenate kinase; MtPanK, *Mycobacterium tuberculosis* pantothenate kinase; N5-Pan, N-pentylpantothenamide; Np-Pan, N-pyridin-3-ylmethylpantothenamide; PanK, pantothenate kinase; RMSD, root mean square deviation

Grant sponsor: Defense Medical Research and Development Program FY10 Basic Research Award; Grant number: DM102976; Grant sponsor: The Structural Genomics Consortium; Grant number: 1097737; Grant sponsors: Canadian Institutes for Health Research, Canadian Foundation for Innovation, Genome Canada through the Ontario Genomics Institute, GlaxoSmithKline, Karolinska Institutet, Knut and Alice Wallenberg Foundation, Ontario Innovation Trust, Ontario Ministry for Research and Innovation, Merck and Co., Inc., Novartis Research Foundation, Swedish Agency for Innovation Systems, Swedish Foundation for Strategic Research, and Wellcome Trust, National Cancer Institute; Grant number: Y1-CO-1020; Grant sponsor: National Institute of General Medical Sciences; Grant number: Y1-GM-1104; Grant sponsor: UChicago Argonne; Grant sponsor: LLC, for the United States Department of Energy, Office of Biological and Environmental Research; Grant number: DE-AC02–06CH11357.

*Correspondence to: Hee-Won Park, Tulane University School of Medicine, Department of Biochemistry and Molecular Biology, 1430 Tulane Ave., Rm. 8543, New Orleans, LA 70112. E-mail: hpark1@tulane.edu

Received 28 November 2012; Revised 5 March 2013; Accepted 7 March 2013
Published online 30 March 2013 in Wiley Online Library (wileyonlinelibrary.com).
DOI: 10.1002/prot.24290

INTRODUCTION

Coenzyme A (CoA), the major acyl group carrier, is essential in multiple metabolic pathways including the citric acid cycle and fatty acid biosynthesis.[1] CoA is synthesized in five steps, starting with the phosphorylation of pantothenate (vitamin B_5) to produce 4′-phosphopantothenate by pantothenate kinase (PanK).[2] In bacteria, the phosphorylated intermediate is then sequentially conjugated with a cysteine, and decarboxylated by the bifunctional 4′-phosphopantothenoyl cysteine synthetase/decarboxylase. In humans, these two reactions are catalyzed by two monofunctional enzymes. The resulting 4′-phosphopantetheine is adenylated by phosphopantetheine adenyltransferase to produce dephospho-CoA, which is subsequently phosphorylated by dephospho-CoA kinase to yield CoA. The components of the CoA biosynthesis pathway constitute attractive targets for drug discovery due to the low sequence similarity between the essential pathway enzymes in humans and their bacterial counterparts.[3] PanK is a practical point of pharmacological intervention because its substrate pantothenate is readily taken up by a pantothenate-specific permease in bacteria.[4]

Among the classes of pantothenate analogues, the N-substituted pantothenamides are noted for their potent cytotoxicity against pathogenic bacteria such as *Escherichia coli* and *Staphylococcus aureus*. The full mechanism underlying the antimicrobial activity of these pantothenate analogues remains unclear. Much of the work in this field has been to elucidate the actions of pantothenamides in *E. coli*. These substrate analogues can be efficiently converted to CoA derivatives using the enzymes of the CoA synthesis pathway[5]; for example, N-pentylpantothenamide (N5-Pan) can be converted to ethyldethia-CoA approximately 10.5 times faster than the rate at which CoA is made from pantothenate. Furthermore, the apo form of acyl carrier protein (ACP) can be modified into inactive ethyldethia-ACP, the accumulation of which can block fatty acid synthesis.[6] However, the inactive ACP can be readily processed by ACP phosphodiesterase back to apo-ACP.[7] In addition, supplementing exogenous fatty acids does not offer full resistance to N5-Pan in *Streptococcus pneumoniae*.[6] These findings suggest that the inhibition of fatty acid biosynthesis may not be the sole mechanism underlying the antimicrobial action of N-substituted pantothenamides. More studies are required to fully uncover the cellular targets of pantothenamides.

Currently, limited PanK structural data deter the potential of pantothenate analogues as a novel antimicrobial strategy. We present the crystal structure of KpPanK (from the multidrug-resistant bacterium *K. pneumoniae*) in complex with N5-Pan at 2.1 Å resolution. The pentyl tail is located in a hydrophobic pocket containing multiple aromatic residues, as previously modeled in EcPanK.[8] On the basis of this finding, we synthesized a pantothenamide, Np-Pan, containing a pyridyl group that can form π–π interactions with the aromatic residues in the hydrophobic pocket. The structure of the KpPanK·Np-Pan complex at 1.95 Å resolution reveals alternate conformations of the pyridyl moiety of Np-Pan in two different molecules of the asymmetric unit. These structural data provide the basis for the design of compounds with improved binding affinities for KpPanK.

MATERIALS AND METHODS

Protein expression and purification

The gene encoding the full-length protein (from *K. pneumoniae* strain 342, residues 1–316) was PCR-amplified and ligated to the pET28-MHL expression vector that encodes an N-terminal hexahistidine tag (GenBank accession EF456735). The resulting plasmid was transformed into *E. coli* BL21(DE3) (Stratagene) competent cells by heat shock. Transformants were initially grown 16 hours overnight at 37°C in Luria Bertani broth (Sigma). The overnight culture was then transferred to Terrific Broth (Sigma) and further grown at 37°C until OD_{600} reached 0.7, followed by overnight induction at 18°C with 1 mM isopropyl β-D-thiogalactopyranoside. The cells were pelleted by centrifugation and resuspended in buffer A (50 mM Tris-HCl pH 8.0, 300 mM NaCl, 5% glycerol) supplemented with 5 mM imidazole, 0.5% 3-[(3-cholamidopropyl)dimethylammonio]-1-propanesulfonate (Sigma), 1 mM benzamidine (Sigma), 1 mM phenylmethanesulfonyl fluoride (Sigma), and 5 units/mL benzonase nuclease (Novagen). Cells were lysed by sonication and the lysate was clarified by centrifugation (16000 rpm, 38351 g) and loaded onto nickel-nitrilotriacetic acid resin beads (Qiagen). Buffer A containing 30 mM and 500 mM imidazole was used to wash the beads and elute the protein, respectively. The protein was further purified on a Superdex 75 column (GE Healthcare) pre-equilibrated with 20 mM Tris-HCl pH 8.0, 5% glycerol, and 200 mM NaCl. To remove co-purified substrates, the protein was dialyzed for 3 days at 4°C in 20 mM Tris-HCl pH 8.0, and stored in the dialysis buffer. The protein was concentrated to 35 mg/mL by centrifugation (3750 rpm, 3267 g) using centrifugal filter units (Amicon, 15 mL size with 10-kDa cutoff) and stored at −80°C until further use.

Crystal preparation, data collection, and structure determination

The protein was incubated overnight at 4°C with 30 mM ADP, 5 mM $MgCl_2$, and 30 mM of either N5-Pan or Np-Pan (see Supporting Information for procedures on the synthesis of pantothenamides). 0.5 μL each of protein stock and reservoir solutions from in-house screening kits were mixed in 96-well Intelli-plates (Art Robbins; Hampton Research) and crystallized using the

Table I
Data Collection and Refinement Statistics for KpPanK Crystals

Ligand	N5-Pan	Np-Pan
PDB ID	4F7W	4GI7
Data Collection		
Beamline	19-ID Advanced Photon Source (APS)	23-IDB (APS)
Wavelength (Å)	0.97931	1.03321
Resolution (Å)	48.04-2.05	40-1.95
Space Group	$P2_12_12_1$	$P2_12_12_1$
No. of molecules in asymmetric unit	8	8
Unit cell parameters (Å)	$a = 127.8$, $b = 130.8$, $c = 190.2$	$a = 127.9$, $b = 130.9$, $c = 193.0$
No. of measured reflections[a]	1,327,648 (181,294)	1,668,077 (214,666)
No. of unique reflections	187,519 (27,124)	234,904 (33,760)
Completeness (%)	99.7 (99.3)	99.9 (99.1)
Friedel Redundancy	7.1 (6.7)	7.1 (6.4)
R_{merge} (%)	14.8 (89.8)	12.9(85.2)
Average I/σ	13.7 (3.0)	9.3 (2.1)
Refinement		
Resolution (Å)	40.0–2.1	40–1.95
R_{work}/R_{free} (%)	18.5/22.6	18.6/22.0
No. of atoms		
Protein	19916	19,886
Ligand/ion	396	381
Water	987	1024
Average B-factors (Å^2)		
Protein	27.5	33.3
Ligand/ion	24.9	32.7
Water	25.9	32.7
RMSD bond length (Å)	0.013	0.010
RMSD bond angle (degrees)	1.4	1.4
Ramachandran Analysis[b]		
Favored (%)	97.7	97.8
Outliers (%)	None	None

[a]Numbers in parentheses are for the outer shell.
[b]Geometric analyses were performed using the Molprobity server.[14]

sitting drop, vapor diffusion method at 18°C. Crystals were initially grown in a solution containing 20% PEG3350 and 0.2 M tri-lithium citrate. The addition of 0.2 μL (±)−1,3-butanediol and 2,5-hexanediol (Hampton Research Additive Screen) to the above protein-buffer mixture improved the diffraction quality of protein crystals containing bound N5-Pan and Np-Pan, respectively. Crystals grew to a size of ~0.1 mm x 0.1 mm x 0.08 mm within a week before they were cryoprotected in a 1:1 mixture of paratone-N and mineral oil, and flash frozen in liquid nitrogen for data collection.

Data collection was carried out using the beamlines 19ID and 23ID-B at the Argonne National Laboratory (Advanced Photon Source). All data were processed using the XDS[9] and the Pointless and Scala programs[10] of the CCP4 program suite.

The crystal structures of KpPanK in complex with N5-Pan and Np-Pan were solved by molecular replacement using the program PHASER[11] and the EcPanK structure as a search model (PDB: 1SQ5). The models went through multiple rounds of model building, refinement, and geometric validation using COOT,[12] Refmac5,[13] and Molprobity,[14] respectively. The structures were refined using simple scaling and isotropic B-factor refinement. All riding hydrogen atoms were generated for geometry and structure factor calculation but omitted from the output coordinates. Water molecules were added through automated building in COOT, and any unmodeled molecules were subsequently added by visual inspection. Uninterpretable densities were modeled as unknown (UNX) atoms. Restraints of N5-Pan and Np-Pan used for refinement were generated using the PRODRG server.[15] Statistics for data collection and refinement are given in Table I. Both the KpPanK structures have been deposited in the Protein Data Bank with the accession codes 4F7W and 4GI7.

All figures were generated using PyMOL (The PyMOL Molecular Graphics System, Version 1.5.0.3, Schrödinger, LLC).

RESULTS AND DISCUSSION

Structural overview

Both the structures of KpPanK in complex with N5-Pan and Np-Pan belong to space group $P2_12_12_1$ and contain eight molecules per asymmetric unit, comprising four homodimers (molecules AC, BD, EF, GH). The final models of KpPanK with bound N5-Pan and Np-Pan were refined to 2.1 Å and 1.95 Å, respectively, and

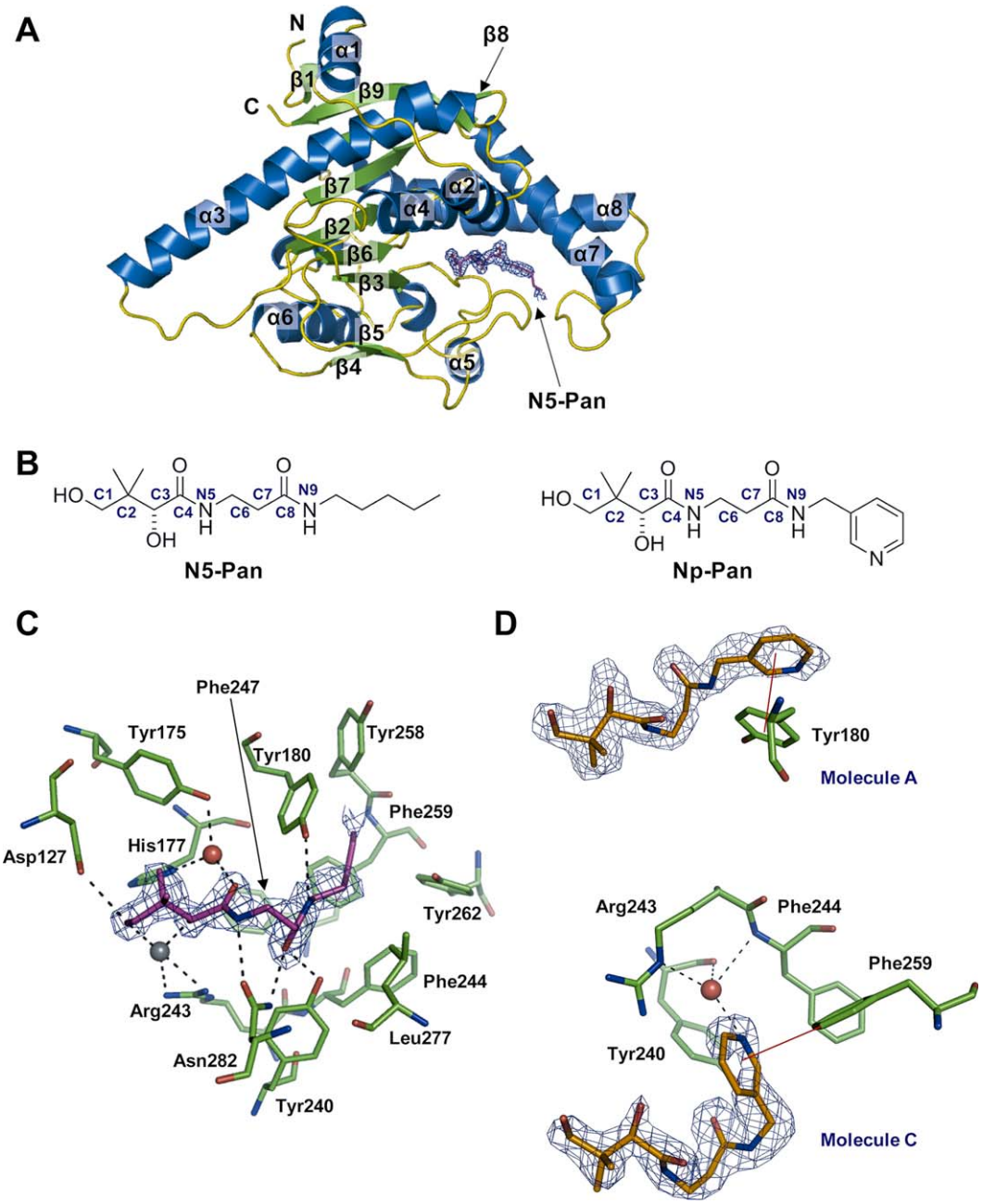

Figure 1

The pantothenamide-binding site of KpPanK. **A**: Ribbon representation of one KpPanK molecule. Helices (blue) and strands (green) and one N5-Pan molecule (magenta) are indicated. The difference map calculated using the Fourier coefficients $F_o - F_c$ is contoured at 2.5σ. **B**: Chemical structures of N5-Pan and Np-Pan. Numbering of the atoms in the pantothenate moiety is shown. **C**: The N5-Pan binding site of KpPanK. N5-Pan (carbon, magenta) and its binding residues of KpPanK (carbon, green) are shown. Dashed lines represent polar interactions of N5-Pan with KpPanK. Water (red sphere) and an unknown atom (gray sphere) are shown. The difference map corresponding to the N5-Pan density is contoured at 2.5σ. **D**: Alternative conformations of Np-Pan. The two observed conformations of Np-Pan (carbon, orange) from molecules A and C are shown in top and bottom panels, respectively. The red lines indicate π-π interactions of the Np-Pan pyridyl ring with Tyr180 of molecule A and Phe259 of molecule C in the sandwich and T-shaped configurations, respectively. The dash lines indicate the water-mediated hydrogen bonds. The difference maps for the Np-Pan density in both panels are contoured at 2.5σ. [Color figure can be viewed in the online issue, which is available at wileyonlinelibrary.com]

include residues 9–316. All molecules are superimposeable and adopt a three layer α-β-α fold made up of eight α-helices and nine β-strands (Fig. 1A). ADP and $MgCl_2$ were included for crystallization, and the initial Fourier difference map showed visible electron density corresponding to ADP but not the Mg^{2+} ion.

The pantothenamide binding pocket of KpPanK

To understand the interactions of KpPanK with N5-Pan at atomic level, we solved the structure of the KpPanK·N5-Pan complex. After modeling water molecules and several rounds of refinement, the F_o–F_c difference map showed clear density for N5-Pan up to the third carbon atom of the pentyl chain for most molecules [Fig. 1(A)]. N5-Pan fits within a pocket defined by parts of helices 7 and 8, and loops β2-α4 (P loop), β3-α5, β4-β5, α5–α6 and α7–α8. The pantothenate moiety is stabilized primarily by polar contacts [Fig. 1(C)]. The C1-hydroxyl forms a hydrogen bond with the Asp127 side chain. Unidentified density was modeled as an unknown atom and is within hydrogen bond distances of the C1 and C3 hydroxyl groups, Arg243, two water molecules and the β-phosphate oxygen. There is a water-mediated hydrogen bond between the C4 carbonyl and His177. Asn282 forms hydrogen bonds with the N5 nitrogen and the C8 carbonyl, which also makes a hydrogen bond with Tyr240. The pentyl tail bends away from Leu277 and the surface of the protein into a hydrophobic pocket made up of several aromatic residues of the α7–α8 loop, which include Tyr180, Tyr240, Phe244, Phe247, Tyr258, Phe259, and Tyr262 [Fig. 1(C)]. The elucidation of the aromatic pocket for the N5-Pan pentyl moiety led us to synthesize a compound, Np-Pan, in which a pyridyl substituent replaces the pentyl group of N5-Pan.

To compare the binding modes of Np-Pan and N5-Pan, we solved the structure of the KpPanK·Np-Pan complex. Visible electron density for the ligand was seen in molecules A, B, C, D, and F, but not for molecules E, G, and H. Molecules A and C showed the clearest electron density for Np-Pan, and were chosen for further analysis. The overall conformations of the Np-Pan binding site of both molecules (A and C) are nearly identical, with slight positional shifts in residues Leu178, Phe247, and Tyr258. The electron density of the pyridine ring is incomplete in the molecules A and C, indicating some disorder is present [Fig. 1(D), top and bottom panels]. In molecule A, the pyridine ring points to the same direction as that of the N5-Pan pentyl moiety, forming a "sandwich" π–π stacking interaction with Tyr180 [Fig. 1(D), top panel]. In molecule C, however, the ring bends in the direction of Arg243, forming a T-shaped/herring-bone π–π interaction with Phe259 [Fig. 1(D), bottom panel]. The pyridyl nitrogen atom in this second conformation is also involved in water-mediated hydrogen bonds with the Tyr240 carbonyl oxygen, the Phe244 amide nitrogen, and the Arg243 side chain guanidinium [Fig. 1(D), bottom panel]. The Y-shaped architecture of the aromatic pocket explains the partial disordering of the pyridine ring; the ring may swing back and forth between the two conformations in the Y-shaped cleft. This finding suggests that the introduction of a second aromatic ring could potentially improve binding further.

Comparison to the substrate-binding site of EcPanK

The residues of KpPanK that interact with pantothenate and form the aromatic pocket are conserved in EcPanK, as we expected based on the highly conserved sequence (90% sequence identity) and structure similarities between KpPanK and EcPanK in complex with pantothenate (PDB: 1SQ5) [Fig. 2(A)] (0.75 Å RMSD for 291 equivalent Cα atoms).[8] Despite the conserved pantothenate-binding site, the pantothenate moiety of N5-Pan of KpPanK has a different mode of binding from the pantothenate of EcPanK with respect to polar interactions. In EcPanK, His177, thought to be the determinant for the dextrorotatory isomer of pantothenate,[8] directly forms a hydrogen bond with the C3 hydroxyl group of pantothenate via the Nϵ nitrogen. In KpPanK, however, the imidazole exists in a different rotamer conformation such that the Nδ nitrogen forms a water-mediated hydrogen bond to the C4 carbonyl of N5-Pan. If His177 of KpPanK were in the same rotamer conformation as in EcPanK, the Nϵ nitrogen would be 3.8 Å away from the C3 hydroxyl of N5-Pan [Fig. 2(B)]. Furthermore, the Tyr180 hydroxyl of KpPanK forms a hydrogen bond to the amide nitrogen of N5-Pan, whereas that of EcPanK is 4.2 Å away from the corresponding carboxyl oxygen of pantothenate [Fig. 2(B)]. The β4-β5 strand of EcPanK containing His177 and Tyr180 that is proximal to the pantothenate moiety is shifted towards the periphery relative to KpPanK [Fig. 2(B)]. These subtle structural differences in the substrate-binding pocket may be useful for designing selective agents against either bacterial strain.

The high sequence and structural similarity between KpPanK and EcPanK allows the use of the latter as the reference conformation from which structural changes induced by N-substitutions can be discerned in KpPanK. Compared with EcPanK, Tyr258 of the α7–α8 loop of KpPanK in both the pantothenamide-bound structures underwent the most significant change, as its side chain was rotated ∼50° away from the bound N-substituent moiety that resulted in a movement of the hydroxyl group by 5 Å [Fig. 2(C)]. Asn261 of the α7–α8 loop was also rotated and shifted ∼2.6 Å away from the bound N-substituent [Fig. 2(C)]. The movements of these residues open up the aromatic pocket for occupation by N-substituents. In addition, the residues of the α7–α8 loop show higher temperature factors than the other parts of protein (∼40–50 $Å^2$), suggesting some disordering and flexibility of the loop; this is supported by the fact that the corresponding loop in EcPanK is considered a mobile lid.[8] The space provided by the opening of the aromatic pocket due to flexibility of the α7–α8 loop explains how the pantothenamides are

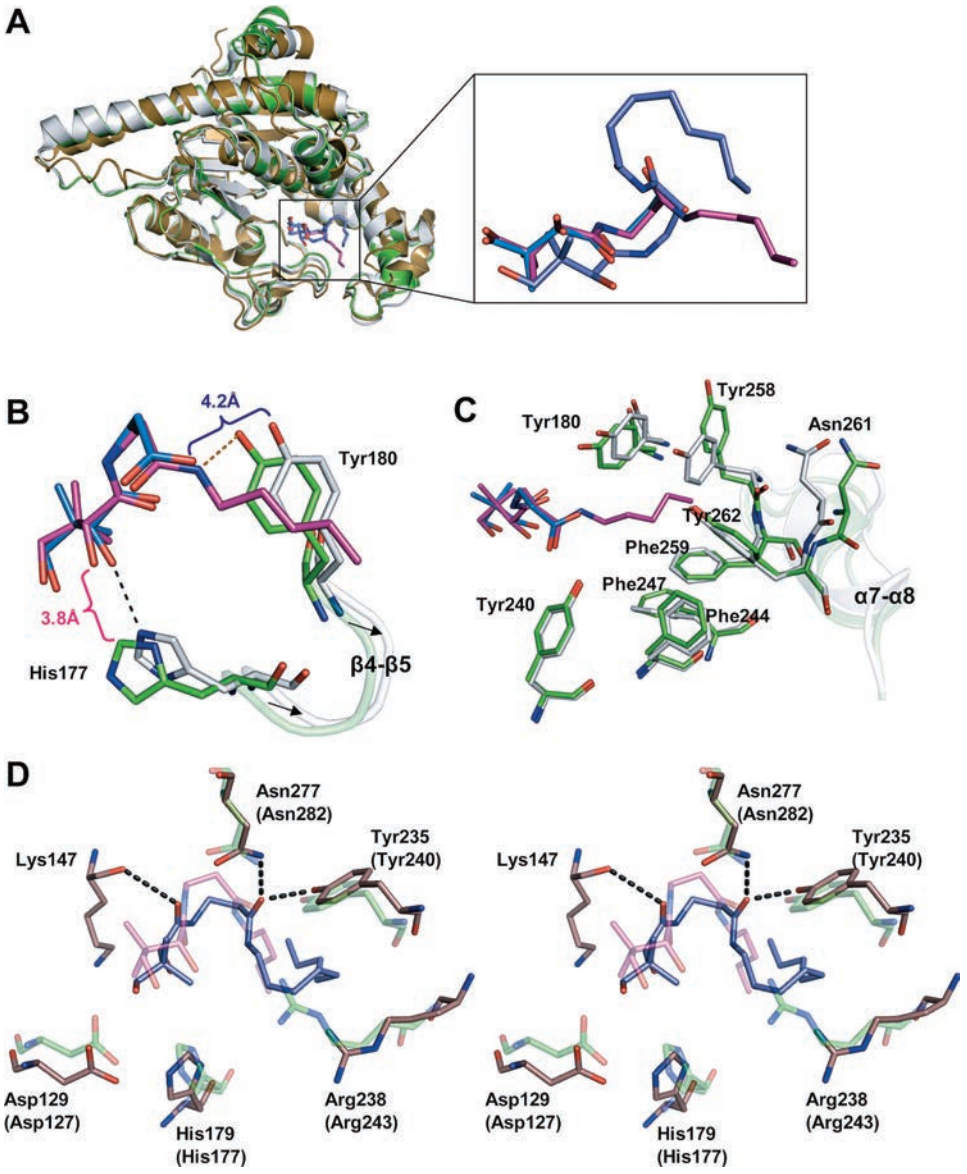

Figure 2

The substrate/pantothenamide binding sites of KpPanK, EcPanK and MtPanK. **A**: Superimposed ribbon representations of KpPanK (green), EcPanK (gray), and MtPanK (brown) molecules. A zoomed-in view of their respective substrates N5-Pan (carbon, magenta), pantothenate (carbon, blue) and N9-Pan (carbon, purple) is shown. **B**: Conformational differences between KpPanK (carbon, green) and EcPanK (carbon, gray) for the residues that interact with the pantothenate moiety of N5-Pan in KpPanK (carbon, purple) and the pantothenate in EcPanK (carbon, blue). Dashed lines indicate hydrogen bonds. Arrows indicate difference in position of the EcPanK β4-β5 loop relative to that of KpPanK. A distance of 3.8 Å indicates no hydrogen bond between the C3 hydroxyl of bound N5-Pan and the Nϵ of His177 in KpPanK, even if the side chain of His177 is flipped to adopt the same rotameric conformation as in EcPanK. Similarly, a distance of 4.2 Å indicates no hydrogen bond between the carboxyl oxygen of bound pantothenate and Tyr180 hydroxyl in EcPanK, different from that observed in KpPanK. **C**: Conformational differences between KpPanK (carbon, green) and EcPanK (carbon, gray) for the residues near the N-pentyl moiety of N5-Pan, which include those of the α7-α8 loop. The enzymes' α7-α8 loops are semi-transparent. **D**: Stereo view of the conformational differences between the complex of KpPanK (carbon, green) and N5-Pan (carbon, magenta) and the complex of MtPanK (carbon, brown) and N9-Pan (carbon, purple). Dashed lines indicate hydrogen bonds between MtPanK and N9-Pan whereas the hydrogen bonds between KpPanK and N5-Pan are not shown for clarity. KpPanK residues are indicated in parentheses.

accommodated by KpPanK to be used as its substrates. Further, the flexible nature of the N-substituent moiety-binding pocket may be exploited in the design of new N-substituted compounds with enhanced binding affinities.

Comparison to the pantothenamide-binding site of MtPanK

The structure of the *Mycobacterium tuberculosis* PanK (MtPanK) in complex with N-nonylpantothenamide

(N9-Pan) is available for comparison (PDB: 3AVQ). KpPanK shares 54% sequence identity with MtPanK and has an RMSD of 1.65 Å for 280 equivalent Cα atoms. All residues involved in binding to the pantothenate moiety are conserved between KpPanK and MtPanK. The corresponding α7–α8 loop residues in MtPanK lining the aromatic pocket are mostly conserved between the two enzymes, with some exceptions as follows (KpPanK residues in parentheses): Met242(Phe247), His253(Tyr258), and H256(N261). Despite high sequence similarities in the ligand binding pockets, the conformations of the bound pantothenamides in the two enzymes are distinct from each other [Fig. 2(D)]. In MtPanK the C3 hydroxyl of N9-Pan is rotated away from the C1 hydroxyl that forms a hydrogen bond to Asp129 of MtPanK whereas in KpPanK the C3 hydroxyl of N5-Pan points toward the same direction as the C1 hydroxyl, of which the position is fixed by its hydrogen bond to Asp127 of KpPanK. The C4 carbonyl of N9-Pan interacts with Lys147 and Asn277 of MtPanK, whereas the same C4 carbonyl of N5-Pan makes a water-mediated hydrogen bonds to Tyr175 and His177 of KpPanK. The N9-Pan C8 carbonyl oxygen interacts with Tyr235 and Asn277, similar to N5-Pan in KpPanK. The N-nonylamino nitrogen of N9-Pan does not interact with any MtPanK protein residue, whereas the corresponding nitrogen of N5-Pan forms a hydrogen bond to Tyr180 of KpPanK. More importantly, the conformation of the nonyl tail of N9-Pan is circularly bent and approaches Arg238 of MtPanK (Arg243 of KpPanK) whereas the pentyl tail of N5-Pan extends towards the protein surface. It is of interest that the bent conformation of the N9-Pan nonyl tail in MtPanK is somewhat similar to that of the pyridine ring of Np-Pan in the molecule C of KpPanK. This finding suggests that pantothenamides with N-ring substituents may bind as well or better to MtPanK than those with long-chained N-alkyl substituents, which needs to be proven by further experiments.

CONCLUSIONS

We have used X-ray crystallography to assess the binding of the two N-substituted pantothenamides, a previously known N5-Pan and a newly synthesized Np-Pan, to KpPanK. These structural studies have identified the flexible, hydrophobic pocket of KpPanK that encases pantothenamide N-substituents, enabling us to design new compounds with higher binding affinities to KpPanK. In addition, comparison of the pantothenamide binding site KpPanK with those of structurally related PanKs, EcPanK, and MtPanK, which share high sequence identities to KpPanK (90 and 54%, respectively), has revealed subtle differences within each compared pair. Exploiting such differences between KpPanK and other PanKs (e.g., from human and nonpathogenic gut flora bacteria) will likely be key to improve pantothenamide selectivity for *K. pneumoniae*.

REFERENCES

1. Lipmann F. On chemistry and function of coenzyme A. Bacteriol Rev 1953;17:1–16.
2. Jackowski S, Rock CO. Regulation of coenzyme A biosynthesis. J Bacteriol 1981;148:926–932.
3. Gerdes SY, Scholle MD, D'Souza M, Bernal A, Baev MV, Farrell M, Kurnasov OV, Daugherty MD, Mseeh F, Polanuyer BM, Campbell JW, Anantha S, Shatalin KY, Chowdhury SA, Fonstein MY, Osterman AL. From genetic footprinting to antimicrobial drug targets: examples in cofactor biosynthetic pathways. J Bacteriol 2002;184:4555–4572.
4. Vallari DS, Rock CO. Pantothenate transport in *Escherichia coli*. J Bacteriol 1985;162:1156–1161.
5. Strauss E, Begley TP. The antibiotic activity of N-pentylpantothenamide results from its conversion to ethyldethia-coenzyme a, a coenzyme a antimetabolite. J Biol Chem 2002;277:48205–48209.
6. Zhang YM, Frank MW, Virga KG, Lee RE, Rock CO, Jackowski S. Acyl carrier protein is a cellular target for the antibacterial action of the pantothenamide class of pantothenate antimetabolites. J Biol Chem 2004;279:50969–50975.
7. Thomas J, Cronan JE. Antibacterial activity of N-pentylpantothenamide is due to inhibition of coenzyme a synthesis. Antimicrob Agents Chemother 2010;54:1374–1377.
8. Ivey RA, Zhang YM, Virga KG, Hevener K, Lee RE, Rock CO, Jackowski S, Park HW. The structure of the pantothenate kinase.ADP.-pantothenate ternary complex reveals the relationship between the binding sites for substrate, allosteric regulator, and antimetabolites. J Biol Chem 2004;279:35622–35629.
9. Kabsch W. Xds. Acta Crystallogr D Biol Crystallogr 2010;66(Part 2):125–132.
10. Evans P. Scaling and assessment of data quality. Acta Crystallogr D Biol Crystallogr 2006;62(Part 1):72–82.
11. Read RJ. Pushing the boundaries of molecular replacement with maximum likelihood. Acta Crystallogr D Biol Crystallogr 2001;57(Part 10):1373–1382.
12. Emsley P, Lohkamp B, Scott WG, Cowtan K. Features and development of Coot. Acta Crystallogr D Biol Crystallogr 2010;66(Part 4):486–501.
13. Murshudov GN, Skubak P, Lebedev AA, Pannu NS, Steiner RA, Nicholls RA, Winn MD, Long F, Vagin AA. REFMAC5 for the refinement of macromolecular crystal structures. Acta Crystallogr D Biol Crystallogr 2011;67(Part 4):355–367.
14. Chen VB, Arendall WB, 3rd, Headd JJ, Keedy DA, Immormino RM, Kapral GJ, Murray LW, Richardson JS, Richardson DC. MolProbity: all-atom structure validation for macromolecular crystallography. Acta Crystallogr D Biol Crystallogr 2010;66(Part 1):12–21.
15. Schuttelkopf AW, van Aalten DM. PRODRG: a tool for high-throughput crystallography of protein-ligand complexes. Acta Crystallogr D Biol Crystallogr 2004;60(Part 8):1355–1363.

PROTEINS
STRUCTURE ■ FUNCTION ■ BIOINFORMATICS

STRUCTURE NOTE

Structural characterization of a new N-substituted pantothenamide bound to pantothenate kinases from *Klebsiella pneumonia* and *Staphylococcus aureus*

Scott J. Hughes,[1] Tetyana Antoshchenko,[2] Kyung Phil Kim,[2] David Smil,[3] and Hee-Won Park[2]*

[1] Department of Pharmacology, University of Toronto, Toronto, Ontario M5G 1L7

[2] Department of Biochemistry and Molecular Biology, Tulane School of Medicine, New Orleans, Louisiana 70112

[3] Structural Genomics Consortium, University of Toronto, Toronto, Ontario M5G 1L7

ABSTRACT

Pantothenate kinase (PanK) is the rate-limiting enzyme in Coenzyme A biosynthesis, catalyzing the ATP-dependent phosphorylation of pantothenate. We solved the co-crystal structures of PanKs from *Staphylococcus aureus* (SaPanK) and *Klebsiella pneumonia* (KpPanK) with *N*-[2-(1,3-benzodioxol-5-yl)ethyl] pantothenamide (N354-Pan). Two different N354-Pan conformers interact with polar/nonpolar mixed residues in SaPanK and aromatic residues in KpPanK. Additionally, phosphorylated N354-Pan is found at the closed active site of SaPanK but not at the open active site of KpPanK, suggesting an exchange of the phosphorylated product with a new N354-Pan only in KpPanK. Together, pantothenamides conformational flexibility and binding pocket are two key considerations for selective compound design.

Proteins 2014; 00:000–000.

Key words: coenzyme A biosynthesis; pantothenate substrate analogs; ligand conformational flexibility; novel antibiotic targets; rational design; X-ray crystallography.

INTRODUCTION

The synthesis of coenzyme A (CoA), the major acyl carrier in all life forms, is vital to various reactions in cellular metabolism, including fatty acid biosynthesis, the citric acid cycle and amino acid metabolism.[1] Universal CoA biosynthesis begins with the phosphorylation of pantothenic acid, also known as vitamin B_5, by pantothenate kinase (PanK). There are currently three known types of PanKs, each differing in their structural and kinetic properties. The prototypical is Type I PanK, of which *Escherichia coli* PanK (EcPanK) is the most characterized. Type II PanKs belong to the acetate and sugar kinase/heat shock protein 70/actin (ASKHA) superfamily and, although most prevalent in eukaryotic species, are expressed by several Gram positive bacteria including *Staphylococcus aureus*. Type I and II PanKs share low sequence identity and differ in their susceptibility to feedback inhibition, with the former inhibited by CoA

Additional Supporting Information may be found in the online version of this article.

Project/Performance sites: Tulane School of Medicine and University of Toronto

*Correspondence to: H.-W. Park; Department of Biochemistry and Molecular Biology, Tulane School of Medicine, 1430 Tulane Avenue, #8543, New Orleans, LA 70112. E-mail: hpark1@tulane.edu

Received 15 November 2013; Revised 16 December 2013; Accepted 6 January 2014

Published online 28 January 2014 in Wiley Online Library (wileyonlinelibrary.com). DOI: 10.1002/prot.24524

and its thioesters. As pantothenate phosphorylation is the first and rate-limiting step in CoA biosynthesis, PanK function is an important determinant in CoA-dependent processes essential for cellular growth and division. The functional significance of PanK coupled with known structural differences between human and pathogenic bacterial PanKs has made this enzyme a target for developing novel antimicrobials.[2]

Investigation into the antimicrobial properties of pantothenate analogs began in the 1970s with the synthesis of *N*-pentylpantothenamide (N5-Pan) and *N*-heptylpantothenamide (N7-Pan). Initial studies with N5-Pan and N7-Pan focused on demonstrating growth inhibition of *E. coli*,[3] but this has since extended to *S. aureus*.[4] These *N*-substituted pantothenamides function as pseudo-substrates, as they are phosphorylated by PanK to produce phospho-pantothenamides, which are subsequently utilized downstream of PanK to produce inactive CoA analogs.[3] Accumulation of these analogs leads to inactivation of acyl carrier protein, thus stopping fatty acid biosynthesis and ultimately leading to cell death. Despite the high potency of N5-Pan and N7-Pan, they lack in specificity by virtue of their nondiscriminate inhibition of Type I (*E. coli*) and Type II (*S. aureus)* PanKs. Specificity is critical for avoiding human cytotoxicity and interference with normal intestinal flora. Structural analysis of Types I and II PanKs indicates a small aromatic pocket around the *N*-substituent end of pantothenate that is unique to Type I PanKs. Moreover, the absence of these bulky residues in Type II PanKs may allow for the accommodation of larger *N*-substitutions. Taken together this suggests that although Type I PanKs may interact more readily with an aromatic substitution, there is a size limitation when compared with Type II PanKs. Indeed a recent crystal structure of Np-Pan (a pyridyl-containing pantothenamide) bound to the Type I PanK from *Klebsiella pneumoniae* (KpPanK) confirms that a *small* aromatic substituent forms π–π interactions with residues of the aromatic pocket. However, the lack of a pantothenamide-bound *S. aureus* PanK (SaPanK) structure prevents confirmation of the hypothesis regarding size limitations.

In the current study, we synthesized N354-Pan, a novel pantothenamide containing an *N*-substituted 1,3-benzopyridoxole ring, and co-crystallized it with KpPanK and SaPanK. Analysis of the structures revealed two distinct conformations of N354-Pan bound to SaPanK and KpPanK, as well as a phosphorylated N354-Pan in SaPanK but not in KpPanK. In addition to N354-Pan flexibility contributing to its promiscuous binding to both the enzymes, two PanKs undergo different conformational changes to accommodate the *N*-substitution of N354-Pan. Herein we discuss the consequences of these conformational changes of SaPanK and KpPanK and the importance of ligand flexibility in the rational design of novel pantothenamides.

MATERIALS AND METHODS

Protein expression and purification

Genes encoding for full length SaPanK (strain MSSA476, residues 1–267) and KpPanK (strain 342, residues 1–316) were purchased from GenScript and amplified by PCR. The resulting products were ligated into the pET28-MHL expression vector containing an *N*-terminal hexahistidine tag (GenBank accession EF456735) and subsequently transformed into *E. coli* BL-21(DE3) (Stratagene) competent cells. Successful transformants were grown in Luria Bertani broth (Sigma) for 16 h at 37°C, and then transferred to Terrific Broth (Sigma). Growth at 37°C continued until the OD_{600} reached 0.7, whereupon the temperature was lowered to 18°C and protein expression was induced by the addition of 1 m*M* isopropyl β-D-thiogalactopyranoside. At 16 h postinduction, cells were collected by centrifugation and resuspended in binding buffer (50 m*M* Tris–HCl pH 8.0, 300 m*M* NaCl, 5% glycerol, 5 m*M* imidazole) supplemented with 0.5% 3-[(3-cholamidopropyl)dimethylammonio]-1-propanesulfonate, 1 m*M* benzamidine, 1 m*M* phenylmethanesulfonyl fluoride, and 5 U/mL benzonase nuclease. The cells were lysed by sonification, and the lysate was centrifuged at 15,000 rpm. The supernatant was loaded on to nickel-nitrilotriacetic acid resin beads, washed with binding buffer containing 30 m*M* imidazole, and bound protein was eluted using binding buffer with 500 m*M* imidazole. The eluant was then loaded on to a 26/60 Superdex 200 size exclusion column pre-equilibrated with 10 m*M* Tris–HCl pH 8.5 and 150 m*M* NaCl. Target protein-containing fractions (SaPanK and KpPank) were pooled and concentrated to 15 mg/mL and 9.7 mg/mL, respectively, using 10-kDa centrifugal filter units (Amicon), and then frozen in aliquots at −80°C until further use.

Crystallization, data collection, and structure determination

Protein was incubated with N354-Pan (Supporting Information Materials and Methods), ATP (1:10 molar ratio for each), and 5 m*M* $MgCl_2$ for 1 h at room temperature. Crystallization trials were conducted using the sitting-drop, vapor diffusion method and in-house screening kits, with each 1 μL drop containing a 1:1 ratio of protein and reservoir solution. Drops were set in 96 well Intelliplates and incubated at 16°C until crystal growth was observed. SaPanK crystals (chunky, ∼150 μm in size) were grown in 1.4 *M* sodium citrate, 0.1 *M* HEPES pH 7.5 and 5% ethylene glycol, whereas KpPanK crystals (plates, ∼100 μm in size) were observed in 2 *M* sodium formate and 0.1 *M* Tris–HCl pH 8.5. Crystals were cryoprotected in an equal (1:1) mixture of paratone-N and mineral oil, and flash frozen in liquid nitrogen until data collection.

Data were collected at the Advanced Photon Source 23-IDD beamline at the Argonne National Laboratory in

Chicago, IL. SaPanK data were processed using the programs XDS,[6] Pointless,[7] and Scala,[7] while KpPanK data processing was carried out using the software suite HKL2000 (HKL Research). Both structures were solved by molecular replacement programs in the CCP4 crystallographic suite;[8] KpPanK was solved with MolRep[9] using pantothenamide-bound KpPanK (PDB ID:4GI7) as a search model, while SaPanK was solved with Phaser[10] using AMPNP-bound SaPanK (PDB ID:2EWS) as a search model. Each model underwent multiple rounds of model building and refinement using COOT[11] and Refmac5.[12] Prior to ligand introduction, a single round of simulated annealing was conducted using CNS Solve.[13] This ligand-excluded model was used to generate unbiased Fourier difference maps (Figs. 1 and 2) for N354-Pan. Real-space correlation coefficients (RSCC) for N354-Pan were calculated using the program OVERLAP-MAP from the CCP4 suite.[8] All riding hydrogens were excluded from the output coordinate files but included for refinement. N354-Pan restraints for refinement were generated using the PRODRG server,[14] and geometric validation was carried out with Molprobity.[15] Summary data collection and refinement statistics can be found in Table I. The KpPanK and SaPanK structures have been deposited into the Protein Data Bank with accession codes 4NE2 and 4NB4, respectively. All images were generated using PyMOL (The PyMOL Molecular Graphics System, Version 1.5.0.4 Schrödinger, LLC).

RESULTS AND DISCUSSION

Structure of N354-bound SaPanK

The crystals of SaPanK belong to the space group $P2_1$, with eight molecules in the asymmetric unit forming four biologically relevant dimers (AB, CD, EF, GH). The final model was refined at 2.25 Å resolution. Each subunit of a dimer is composed of two domains (Domains I and II), and a loop region that forms a "binding cap" (residues 153–172). Domain I is composed of a single β-sheet (1; β1–β5) layered between helices α1, α2, and α8. The larger Domain II similarly consists of a single β-sheet (2; β6–β10) between helices α4–α7 and α3 [Fig. 1(a)]. Similar to the previous SaPanK structure (PDB ID: 2EWS), the main dimerization interface is between helices α6 and α'6 on the adjacent subunit. In addition, the

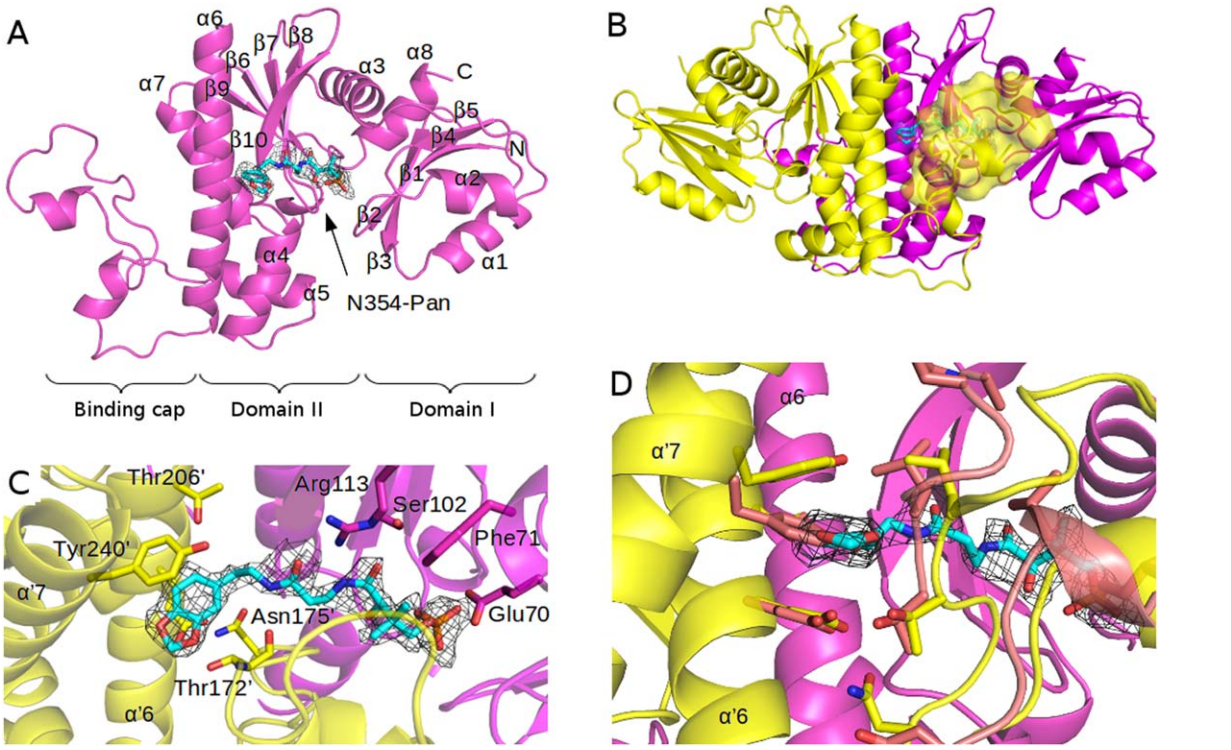

Figure 1

Structure of N354-Pan-bound SaPanK. **a** Representative molecule H from SaPanK structure showing secondary structure elements and the location of the binding site. **b** Representative dimer GH illustrating how the binding cap fits over top of the adjacent subunit. **c** Binding site for the elongated conformation of p-N354-Pan showing interacting residues. The site is composed of residues from both subunits (magenta and yellow). **d** Structural comparison of N354-Pan-bound (magenta) and AMPPNP-bound SaPanK (pink). The 1,3-benzodioxole ring fits into a cavity at the interface between helices α6 and α'6 that is occupied by Tyr240' in the AMPPNP-bound structure. All Fourier difference maps ($F_o - F_c$) are contoured to 2.5σ.

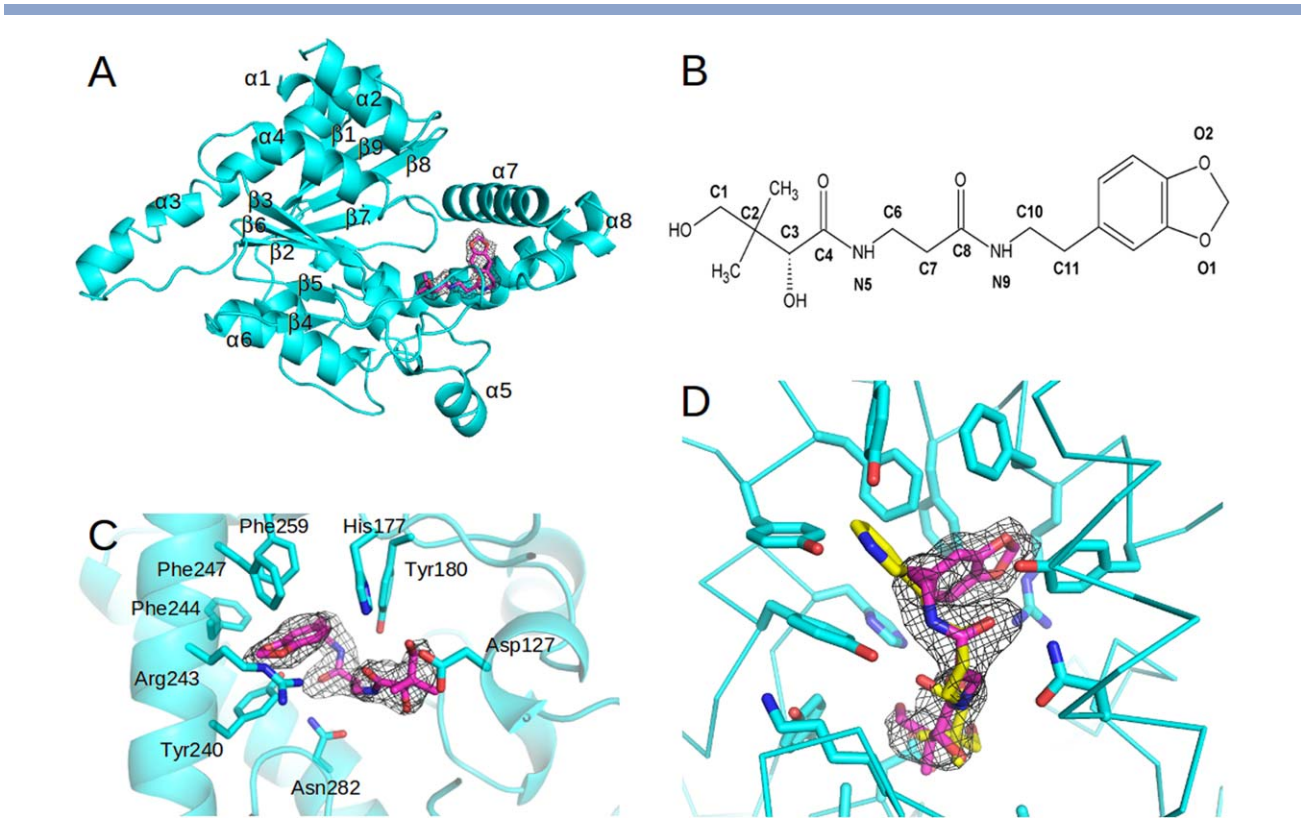

Figure 2

Structure of N354-Pan-bound KpPanK. **a** Representative molecule of KpPanK showing secondary structure elements and the N354-Pan binding sites. **b** Chemical structure of N354-Pan. **c** Binding site for the bent conformation of N354-Pan, showing interacting residues. **d** Overlay of N354-Pan (magenta) and Np-Pan (PDB ID: 4GI7; yellow) illustrating the two aromatic pockets in KpPanK. Np-Pan is able to fit into a smaller pocket formed by Y262, F259, and Y258, whereas N354-Pan must interact with the larger pocket formed by F247, F244, and Y240. All Fourier difference maps ($F_o - F_c$) are contoured to 2.5σ. [Color figure can be viewed in the online issue, which is available at wileyonlinelibrary.com.]

binding cap of one subunit closes over the binding site of the second subunit of the dimer, interacting with β-sheets 1 and 2, and helices α3 and α8 [Fig. 1(b)]. The protein was crystallized in the presence of ATP, N354-Pan and $MgCl_2$, but the Fourier difference map shows density for ADP, Mg^{2+} and phosphorylated N354-Pan (p-N354-Pan). Further description below will focus on the GH dimer with the best density for p-N354-Pan.

In the GH dimer of SaPanK, the p-N354-Pan adopts an elongated conformation so as to rest in a pocket formed by the loops of β1–β2, β4-α2 and β6-β7, helix α3, and strands β6 and β7 with the binding cap from the second subunit of the dimer on top of the p-N354-Pan [Fig. 1(c)]. The pantothenoyl moiety of p-N354-Pan [C1–C8, inclusive, Fig. 2(b)] fits in a hydrophilic groove formed between the β-sheet of β6–β10 and the binding cap. Specific interactions include hydrogen bonding between C4 and C8 carbonyl oxygens and Arg113, between C4 carbonyl oxygen and Ser102, and between N5 and the backbone carbonyl of Thr101. At the phosphorylated end of p-N354-Pan, the catalytic Glu70 is within hydrogen bonding distance of the oxygen bridging the phosphate and C1, and the phosphate forms an extensive hydrogen bond network with a water molecule, Mg^{2+}, Glu70, the backbone carbonyl of Gly100, and the β-phosphate of ADP. The *N*-substituted 1,3-benzodioxole ring of p-N354-Pan binds almost exclusively with the second subunit of the SaPanK dimer. The benzodioxole ring fits into a cavity generated by the binding cap and helices α'7 and α'6, forming a π–π interaction with Tyr240' and hydrogen bond to the backbone carbonyl of Thr172 [Fig. 1(d)].

Structure of N354-Pan-bound KpPanK

The crystals of KpPanK belong to the space group F222 with two molecules in the asymmetric unit. These two molecules in the asymmetric unit do not represent a biologically relevant dimer of KpPanK, which can be assembled by applying a crystallographic twofold symmetry operation to each of the two molecules in the asymmetric unit. The final model was refined to 1.9 Å, and the two molecules are superimposable [root-mean-square deviation (Rmsd): 0.037], each of which contains residues

Table I
Data Collection and Refinement Statistics for PanK Structures

Protein	SaPanK	KpPanK
Ligand	*N*354-Pan	*N*354-Pan
PDB ID	4NB4	4NE2
Data collection		
Beamline	23-IDD Advanced Photon Source (APS)	23-IDD APS
Wavelength (Å)	1.03318	1.03318
Resolution (Å)	40.0–2.25	40.0–1.89
Space group	$P2_1$	F222
No. of molecules in asymmetric unit	8	2
Unit cell parameters (Å, °)	$a = 103.0$, $b = 70.7$, $c = 143.1$, $\beta = 90.6$	$a = 106.8$, $b = 180.4$, $c = 181.5$
No. of measured reflections[a]	405,701 (59,673)	574,166
No. of unique reflections	92,612 (14,133)	65,162 (6898)
Completeness (%)	99.5 (99.2)	99.9 (100.0)
Wilson B factor (Å^2)	16.5	24.8
Friedel redundancy	4.2 (4.2)	8.3 (8.1)
Rmerge (%)[b]	9.4 (30.1)	12.1 (45.3)
Average I/σ	12.4 (5.7)	49.1 (9.0)
Refinement		
Resolution (Å)	40.0–2.25	40.0–1.90
R_{work}/R_{free} (%)[c]	23.0/28.4	15.4/21.1
No. of atoms		
Protein	16,303	5017
Ligand/ion	464	108
Water	476	408
Ligand RSCC[d] (%)	71.0	78.1
Average B factors (Å^2)		
Protein	23	33.3
Ligand/ion	21.7	43.6
Water	18.8	41.4
RMSD bond length (Å)	0.006	0.009
RMSD bond angle (degrees)	1.05	1.27
Ramachandran analysis[b]		
Favored (%)	97.6	98.5
Outliers (%)	None	None

[a]Numbers in parentheses are for the outer shell.
[b]$R_{merge} = \Sigma[(I - <I>)]/\Sigma(I)$, where I is the observed intensity and $<I>$ is the average intensity.
[c]$R_{work} = \Sigma[|F_{obs}| - |F_{calc}|]/\Sigma|F_{obs}|$, where $|F_{obs}|$ and $|F_{calc}|$ are magnitudes of observed and calculated structure factors respectively. R_{free} was calculated as R_{work} using 5.0% of the data, which was set aside for an unbiased test of the progress of refinement.
[d]$RSCC = (<\rho_{obs}\rho_{calc}> - <\rho_{obs}><\rho_{calc}>)/(<\rho_{obs}^2> - <\rho_{obs}>^2)^{1/2}$ $(<\rho_{calc}^2> - <\rho_{calc}>^2)^{1/2}$, where ρ_{obs} and ρ_{calc} represent density values from $F_o - F_c$ maps before and after ligand introduction.

8–316. The overall fold is a typical Rossman-like α-β-α "sandwich", with a 7-stranded mixed β-sheet (strands 1–9-8-7-2–6-3; all parallel except 9) between helices α1–α4 and α5–α8. The dimerization interface is formed by helix α3 and the β6–β7 loop, with the pantothenate binding sites located opposite the interface [Fig. 2(a)].

Although KpPanK was incubated with ATP, $MgCl_2$, and N354-Pan for crystallization, the Fourier difference map showed density for Mg^{2+}, ADP and nonphosphorylated N354-Pan. The binding pocket for N354-Pan lies in a cleft formed by the loops of β3-α5, α5-α6 and β4-β5 and helices α7 and α8. Binding of the pantothenoyl moiety of N354-Pan to KpPanK involves a mixture of polar and nonpolar interactions with KpPanK, whereas the *N*-substituted 1,3-benzodioxole ring of N354-Pan sits near a cluster of aromatic residues (Tyr180, Tyr240, Phe244, Phe247, Tyr258, Phe259, and Tyr262; Fig. 2). The ring substituent bends ~90° with respect to the C1–N9 axis of the pantothenoyl moiety, thus entering a pocket formed by Tyr240, Phe244, Phe247, and Phe259, referred as the N354-Pan-binding pocket of KpPanK [Fig. 2(c)]. Both the KpPanK molecules contain the same bent conformation of N354-Pan, which is consistent with the idea that the elongated conformation observed in SaPanK is disallowed due to steric hindrance imposed by the tight packing of Tyr258, Phe259, and Tyr262. In addition to π–π 'sandwich' stacking with Tyr240 and 'T-shaped' π–π stacking with Phe259, the bent conformation of N354-Pan is further stabilized by a hydrogen bond between O2 of N354-Pan and Arg243. This critical arginine also forms a salt bridge with the β-phosphate of ADP, an interaction important for stabilizing the bound nucleotide. For the pantothenoyl moiety of N354-Pan, Asn282 forms a hydrogen bond with the C8 oxygen, while N9 forms a hydrogen bond with Tyr180. There is also a hydrogen bond between C4 carbonyl of N354-Pan and His177. The C1 end of N354-Pan has weaker density, particularly around the C1 hydroxyl group, suggesting some disordering of this region. Two different side chain rotamers for the catalytic Asp127 have been modeled into molecule B, one of which is within

hydrogen-bonding distance to the C1 hydroxyl group. The alternate conformations observed for the catalytic atom and residue are likely due to the absence of the γ-phosphate in the bound ADP at the active site, the source of the phosphoryl group for the phosphorylation reaction that is initiated by Asp127 deprotonation of the C1 hydroxyl group, followed by a direct nucleophilic attack on the γ-phosphate.

Ligand-induced conformational changes resulting in the closed form of SaPanK and the open form of KpPanK

We have shown that the pantothenate substrate pocket of SaPanK is composed of residues from both the subunits of a dimer, with the groove of one subunit being capped with a loop from the second subunit. Comparison of the N354-Pan-bound SaPanK structure to the AMPPNP-bound structure (PDB ID: 2EWS) offers evidence for both the active site closure that follows the binding of pantothenate substrate or its analog and the mode of closure. In the absence of N354-Pan, the binding cap is disordered in the AMPPNP-bound structure (PDB ID: 2EWS). The N354-Pan can provide complementary hydrogen bond donors (N5, N9) and hydrogen bond acceptors (C4, C8) for the groove and binding cap. Upon the binding of N354-Pan to the groove the binding cap folds over the N354-Pan-bound groove, resulting in the closure of the active site for the phosphorylation reaction.

In contrast to SaPanK, the conformational change that occurs due to pantothenate and its analogs binding to KpPanK is entirely within each subunit of the dimer. There is no KpPanK structure complexed with the nucleotide substrate only or the nucleotide and pantothenate substrates together. However, KpPanK and EcPanK share a high sequence similarity (∼94%) and the available EcPanK structures can therefore be used for the analysis of N354-Pan-induced conformational changes in KpPanK. Comparison of the structures of KpPanK and EcPanK in N354-Pan-bound and Pan-bound states, respectively, shows that they are highly superimposed (Rmsd = 0.535 Å). It has been suggested that pantothenate binding causes conformational changes in EcPanK involving helix α7 and loop α7–α8[5]. Therefore, it is safe to speculate that the binding of N354-Pan to KpPanK would cause similar conformational changes that involve helix α7 and loop α7–α8 to those of EcPanK, creating a channel near the carboxylate of pantothenate, presumably allowing for product exit after the phosphorylation reaction. These conformational changes also facilitate the formation of an aromatic pocket for the binding of the ring substituent of N354-Pan, as several aromatic residues are contributed by the α7–α8 loop. This finding suggests that the N354-Pan-induced conformational changes that are required for the formation of a putative product exit channel as well as for accommodation of the benzodioxole substitution.

Comparison of N354-Pan binding in KpPanK and SaPanK

The structures of N354-Pan-bound SaPanK and KpPanK reported here show how ligand conformational freedom enables the two different binding sites of SaPanK and KpPanK to accommodate the same ligand. In SaPanK, the *N*-substituent on N354-Pan is able to interact with the long cavity in SaPanK by maintaining an elongated conformation. If N354-Pan were restricted to this elongated conformation, one would expect difficulty in the interaction of the benzodioxole substituent with the putative product exit channel of KpPanK, which is shorter than SaPanK due to the presence of several aromatic residues (F259, Y262). However, the ethylene link between the pantothenate and benzodioxole moieties allows N354-Pan to bend, extending the ring substituent sideways into the larger aromatic pocket in KpPanK. This finding suggests that the flexibility of N354-Pan has played a major role in binding to both the PanK proteins, each of which contain binding pockets for the ring substituent of N354-Pan that differ in size and polarity.

Both enzymes contain ADP despite being incubated with ATP for crystallization, but SaPanK is bound to phosphorylated N354-Pan whereas KpPanK contains nonphosphorylated N354-Pan. As bound ADP indicates that N354-Pan acts as a pseudo-substrate in both proteins, the difference in N354-Pan phosphorylation suggests dissimilar mechanisms of product release between SaPanK and KpPanK. Compared to the AMPPNP-bound structure in SaPanK, a shift of helix α'6 and the movement of Tyr240' (4.6 Å away from the binding cap) of the second subunit of a dimer creates a cavity for the benzodioxole ring of N354-Pan [Fig. 1(d)]. The presence of the benzodioxole ring between the binding cap and helix α'6 restricts opening the binding cap in the closed conformation, as it stacks with Tyr240' and forms hydrogen bonds with the backbone of residues in the binding cap. Therefore it is likely that SaPanK undergoes a conformational change to accommodate N354-Pan, but in doing so locks the enzyme in the closed conformation, not releasing p-N354-Pan and halting a catalytic cycle. This is consistent with the presence of p-N354-Pan at the active site of SaPanK. By comparison, in KpPanK the part of bound N354-Pan is visible through the putative product exit channel, implying that N354-Pan leaves the active site via the channel upon phosphorylation in exchange for new N354-Pan. This may explain the presence of N354-Pan and ADP in the KpPanK active site.

Implications for ligand optimization

As evident from the SaPanK and KpPanK structures presented herein, ligand flexibility as well as ligand-binding site polarity and complementarity must be considered when designing novel compounds. Moreover, the

presence of multiple conformers of N354-Pan provides some insight into designing compounds that have improved affinities and selectivity. Structural comparison of KpPanK in complex with three different pantothenamides, N7-Pan, Np-Pan and N354-Pan, reveals that, although none of the three compounds are able to adopt a truly elongated conformation, N7-Pan is accommodated by an aromatic pocket formed by Tyr258, Phe259, and Tyr262. This pocket, referred to as the N7-Pan-binding pocket, is smaller than the N354-Pan-binding pocket. Intriguingly, Np-Pan (PDB ID: 4GI7) can adopt two different rotamer conformations to allow the pyridyl substituent to bind to the N354-Pan-binding and the N7-Pan-binding pockets, respectively. The pyridyl nitrogen also contributes to binding, as it forms a hydrogen bond with Arg243 and Tyr258 in the respective substituent binding pockets [Fig. 2(d)]. This finding suggests that a compound that exploits *both* pockets, that is to say a branched compound containing two heterocyclic aromatic rings, would be more potent than the existing compounds. Furthermore, the branched compound may have difficulty binding to the elongated pocket of SaPanK, reducing affinity toward SaPanK.

On the other hand, a compound that is unable to adopt a bent conformation may enhance activity toward SaPanK. The addition of a double bond within the linker between the pantothenoyl and benzodioxoyl moieties, or the shortening of this linker by one carbon, would force the compound to retain an elongated conformation.

CONCLUSION

In the present study, the crystal structures of N354-Pan-bound SaPanK and KpPanK demonstrate the importance of compound flexibility in the rational design of pantothenamides. Structural comparison predicts the favored interaction of N354-Pan with SaPanK, which consists of a long cavity for the benzodioxole ring that maintains the elongated conformation of N354-Pan. However, KpPanK can interact with a bent conformer of N354-Pan, identifying the importance of compound flexibility. Further optimization should focus on restricting the movement of N354-Pan and designing a branched compound of N354-Pan for SaPanK and KpPanK, respectively. In addition, N354-Pan may actually function as an inhibitor in SaPanK after its initial phosphorylation, as the elongated conformer of N354-Pan extends into the adjacent subunit of the dimer, thereby obstructing the re-opening of the binding cap. The bent conformer of N354-Pan, on the other hand, is able to interact with KpPanK in a similar manner to pantothenate, acting as a pseudo-substrate. In conclusion, N354-Pan flexibility clearly plays a role in selectivity and perhaps enzyme kinetics, and must not be overlooked when designing new improved compounds.

ACKNOWLEDGMENTS

We are thankful to Mr. Jung Hyun Song for his time and effort in the manual validation of the structures. This work was supported by a Defense Medical Research and Development Program FY10 Basic Research Award DM102976 (Hee-Won Park). Results shown in this report are derived from work performed at Argonne National Laboratory, Sector 23-ID at the Advanced Photon Source. The ANL is operated by UChicago Argonne, LLC, for the U.S. Department of Energy, Office of Biological and Environmental Research under contract DE-AC02–06CH11357.

REFERENCES

1. Begley TP, Kinsland C, Strauss E. The biosynthesis of coenzyme A in bacteria. Vitam Horm 2001;61:157–171.
2. Spry C, Kirk K, Saliba KJ Coenzyme A biosynthesis: An antimicrobial drug target. FEMS Microbiol Rev 2008;32:56–106.
3. Clifton G, Bryant SR., Skinner CG. N'-(substituted) pantothenamides, antimetabolites of pantothenic acid. Arch Biochem Biophys 1970;137:523–528.
4. Choudhry AE, Mandichak TL, Broskey JP, Egolf RW, Kinsland C, Begley TP, Seefeld MA, Ku TW, Brown JR, Zalacain M, Ratnam K. Inhibitors of pantothenate kinase: novel antibiotics for staphylococcal infections. Antimicrob Agents Chemother 2003;47:2051–2055.
5. Leonardi R, Chohnan S, Zhang YM, Virga KG, Lee RE, Rock CO, Jackowski S. A pantothenate kinase from *Staphylococcus aureus* refractory to feedback regulation by coenzyme A. J Biol Chem 2005; 280:3314–3322.
6. Kabsch W. XDS. Acta Crystallogr D Biol Crystallogr 2010;66:125–132.
7. Evans PR. Scaling and assessment of data quality. Acta Crystallogr D Biol Crystallogr 2006;62:72–82.
8. Potterton E, Briggs P, Turkenburg M, Dodson E. A graphical user interface to the CCP4 program suite. Acta Cryst 2003;D59:1131–1137.
9. Vagin A, Teplyakov A. MOLREP: An automated program for molecular replacement. J Appl Crystallogr D 1997;30:1022–1025.
10. McCoy AJ, Grosse-Kunstleve RW, Adams PD, Winn MD, Storoni LC, Read RJ. Phaser Crystallographic Software. J Appl Crystallogr D 2007;40:658–674.
11. Emsley P, Cowtan K. Coot: Model-building tools for molecular graphics. Acta Crystallogr D Biol Crystallogr 2004;60:2126–2132.
12. Murshudov GN, Vagin AA, Dodson EJ. Refinement of macromolecular structures by the maximum-likelihood method. Acta Crystallogr D Biol Crystallogr 1997;53: 240–255.
13. Clore GM, Delano WL, Gros P, Grosse-Kunstleve RW, Jiang J-S, Kuszewski J, Nilges M, Pannu NS, Read RJ, Rice LM, Simonson T, Warren GL. Crystallography and NMR system (CNS), a new software suite for macromolecular structure determination. Acta Crystallogr D Biol Crystallogr 1998;54:905–921.
14. Schüttelkopf AW, van Aalten DMF (2004) PRODRG—A tool for high-throughput crystallography of protein–ligand complexes. Acta Crystallogr D Biol Crystallogr 60: 1355–1363.
15. Arendall WB 3rd, Headd JJ, Keedy DA, Immormino RM, Kapral GJ, Murray LW, Richardson JS, Richardson DC. MolProbity: All-atom structure validation for macromolecular crystallography. Acta Crystallogr D Biol Crystallogr 2010;66:12–21.

Supporting Data

Figure 1. SaPanK structure
Left, phosphorylation of N5-Pan in the presence of ATP. The coupled phosphate group of bound Pho-N5-Pan molecule was indicated in a dotted-circle line.

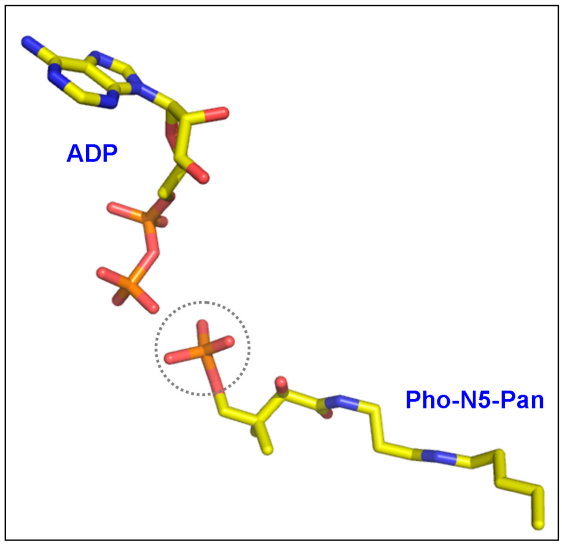

Right, interaction of p-N5-Pan with surrounding residues. The bound p-N5-Pan (yellow) and interacting residues were represented in a ball and stick model. The hydrophilic interactions were indicated by dotted lines.

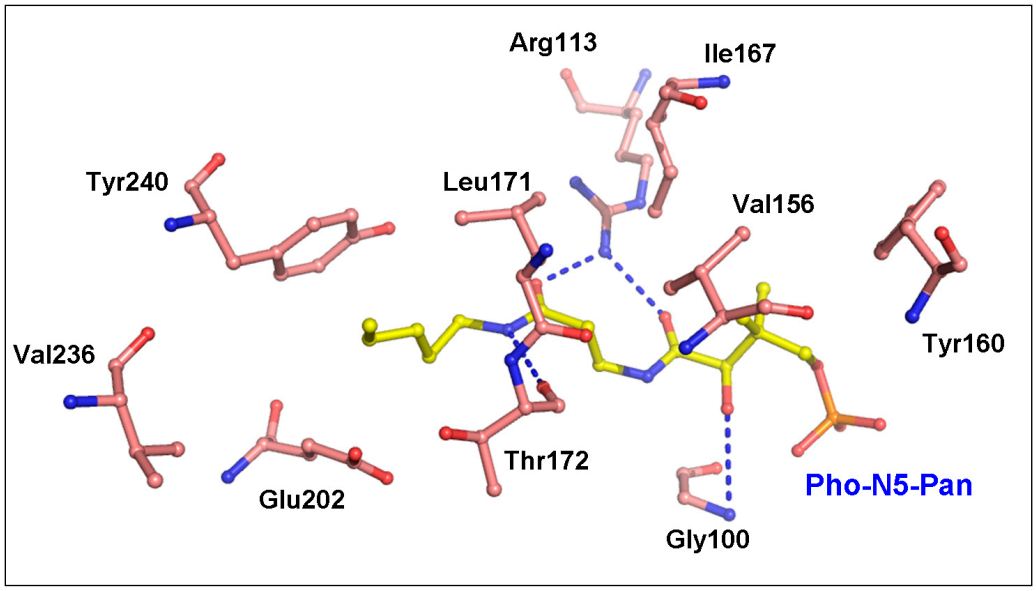

Figure 2. Superimposed view of bound two phosphorylated pantothenate analogs and surrounding residues. Pho-N5-Pan and Pho-N7-Pan were colored yellow and cyan, respectively. The surrounding residues from Pho-N5-Pan and Pho-N7-Pan bound SaPanK were shown in skin and green color ball-and-stick models.

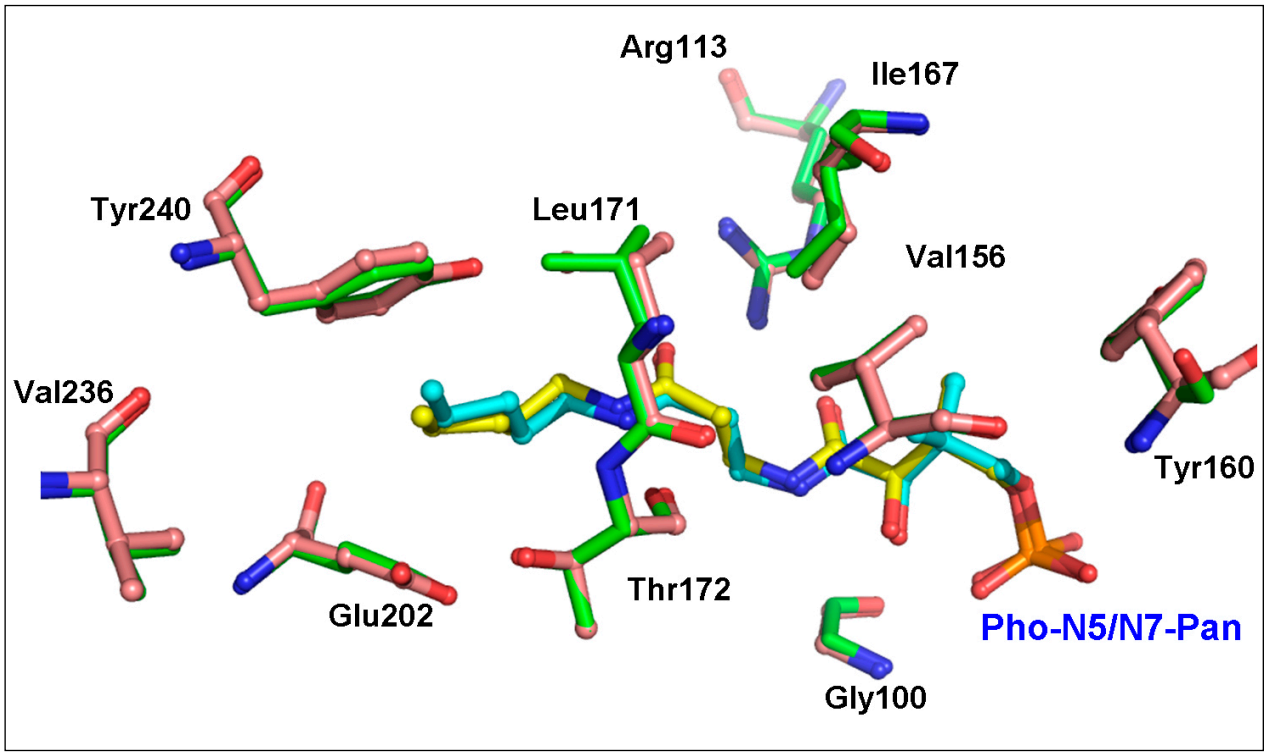

Figure 3. The N7-binding sites of PanKs. *Left,* the N7 moiety (green) is bound by polar residues, W341, R306 and S303 and N299 of hPanK3. *Right,* the N7-moiety (green) is bound by hydrophobic residues, Y258, F259, F247, F244 and Y240.

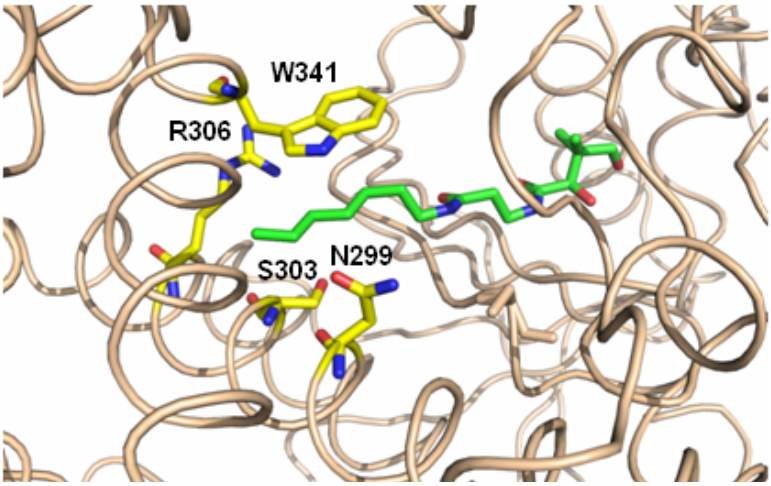

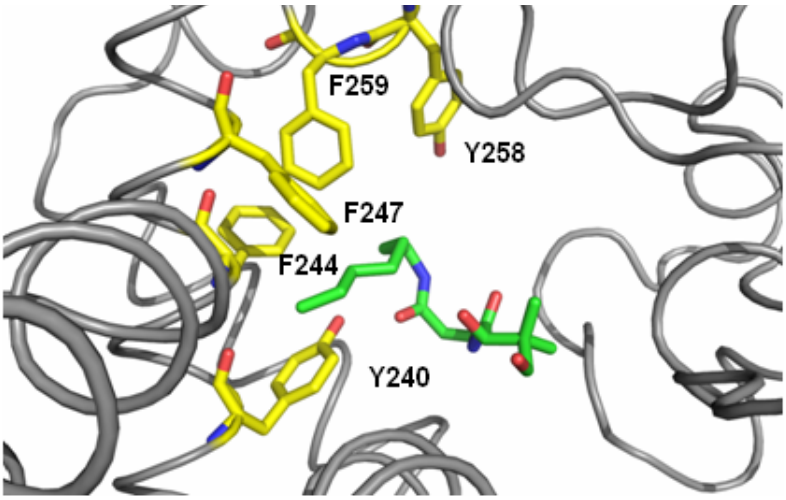

Figure 4. Co-crystal structures of KpPanK and EcPanK with N5-Pan. *Left,* both the structures of KpPanK and EcPanK are dimeric (green and cyan). N5-Pan is bound to only one molecule. *Right,* a zoomed-in view of the N5-Pan binding site of EcPanK shows the bending of N5, similar to that of KpPanK. Non-polar aromatic residues of EcPanK interacting with the pentyl moiety of N5-Pan are labeled.

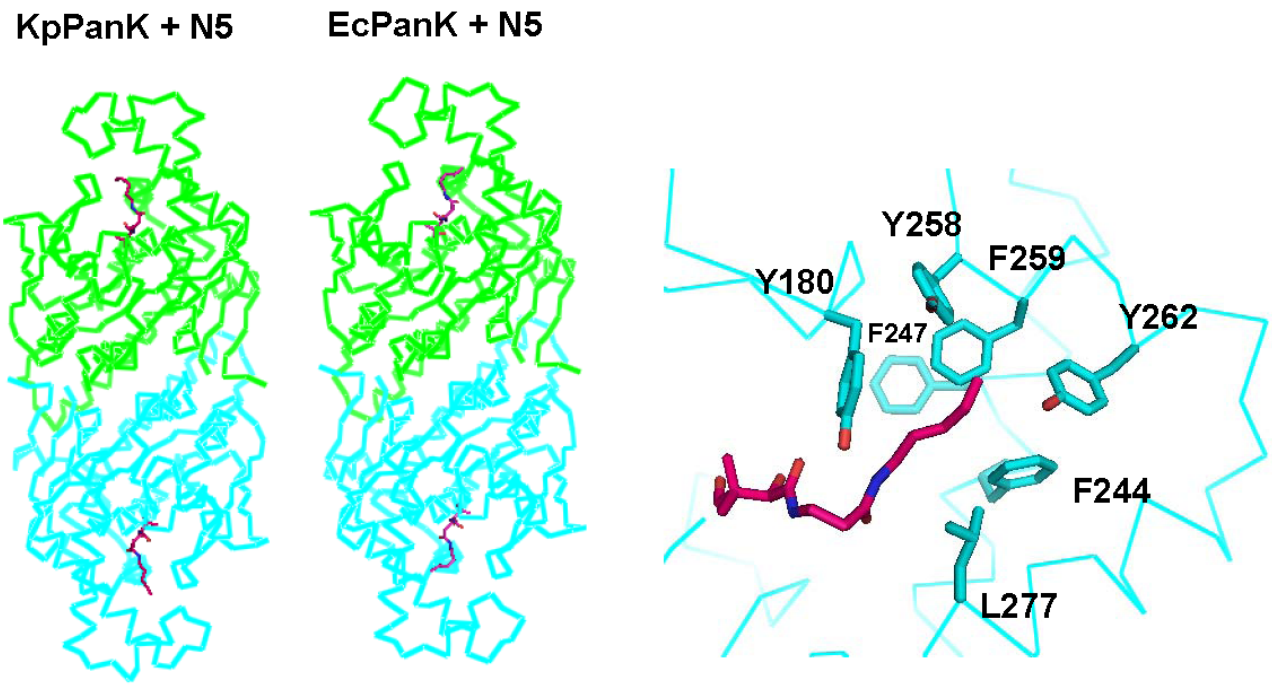

Figure 5. Overall structure of dimeric Human PanK3 complexed with N7-Pan. The bound Pan-analog was presented in a space-filling model.

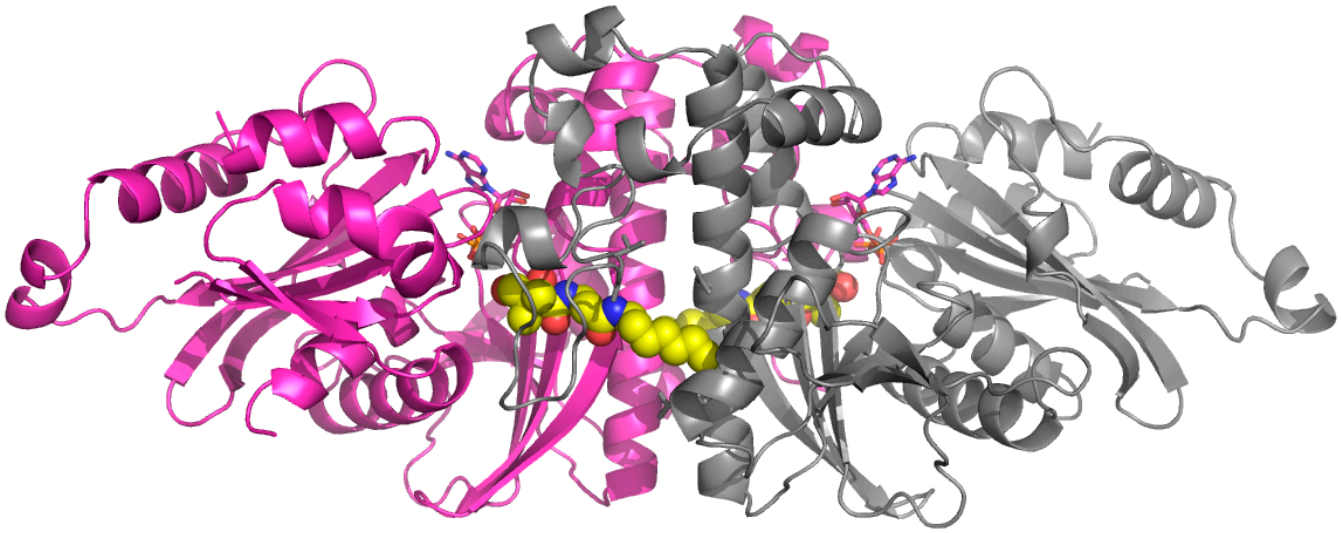

Figure 6.
Left. Structural superimposition of N7-Pan bound SaPanK (cyan) and hPanK3 (magenta).

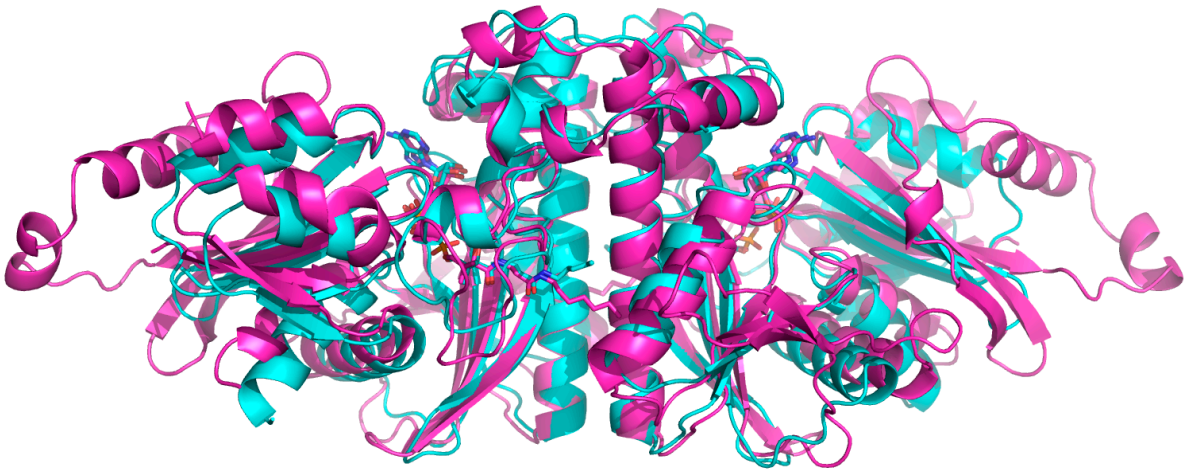

Middle, zoomed view of overlapped N7-Pan analogs from SaPanK (cyan) and hPanK3 (magenta).

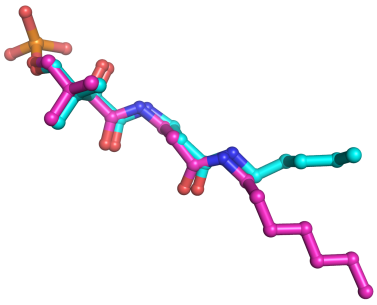

Right, difference in the interaction mode of N7-Pan analogs observed between SaPanK (cyan) and hPanK3 (magenta).

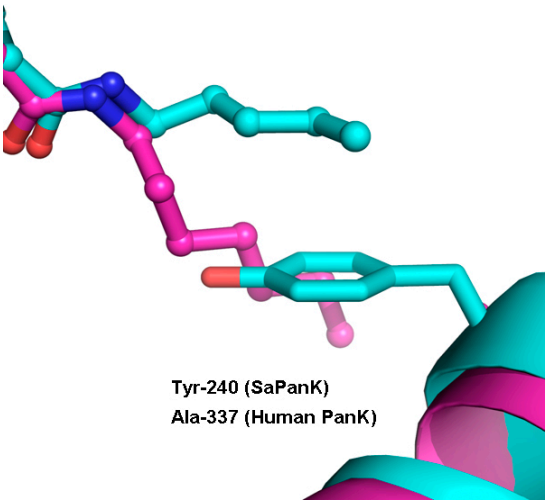

Figure 7. A new set of Pan analogs including MT-0183 and MT-0190 as well as N5-Pan (MT-182) and N7-Pan (MT-181)

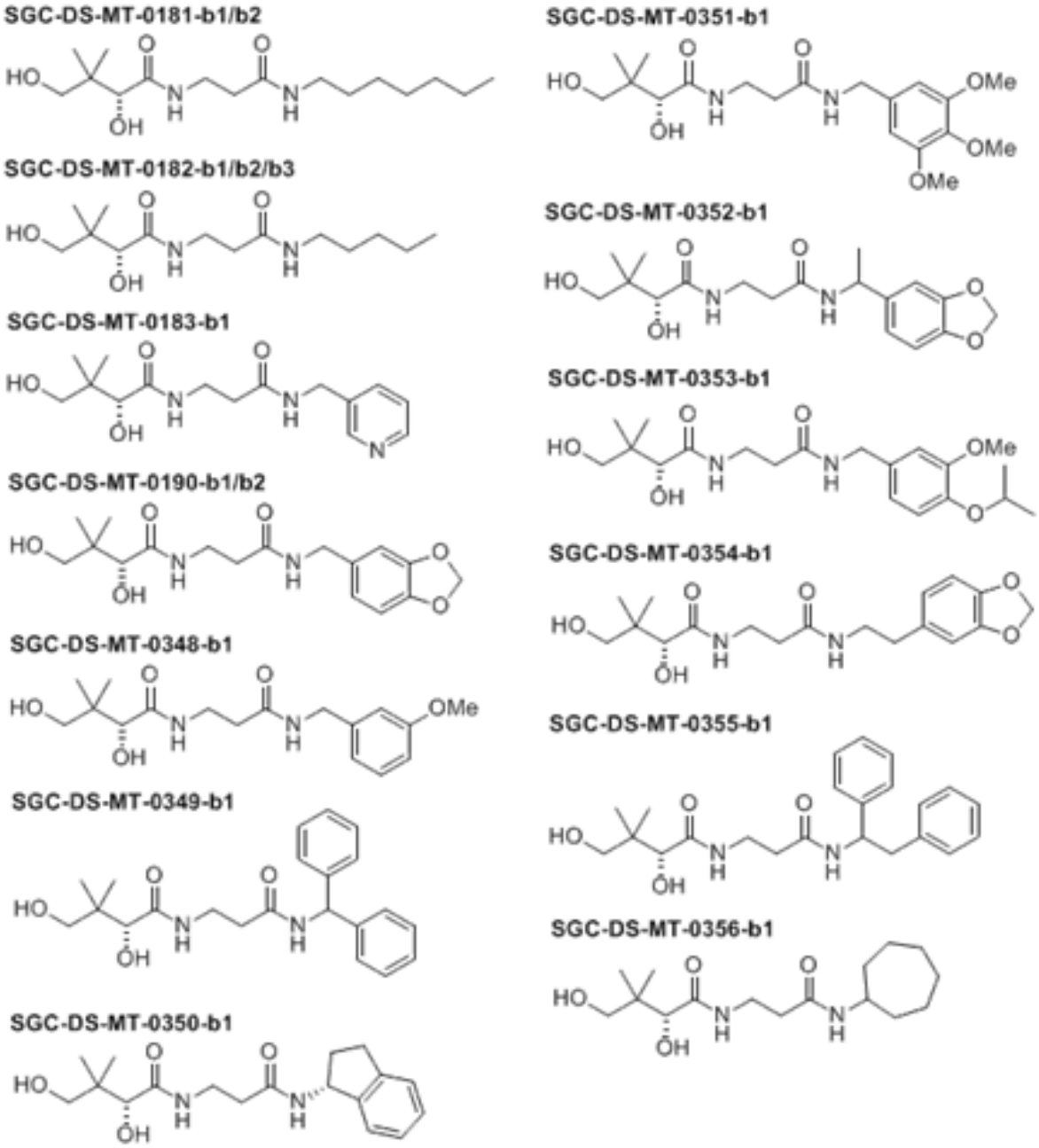

Figure 8. Relative activities of recombinant pantothenate kinases. The activities are normalized to that of SaPanK. Ec: EcPanK, Kp: KpPanK, Sa: SaPanK, Hu2: hPanK2, Hu3: hPanK3.

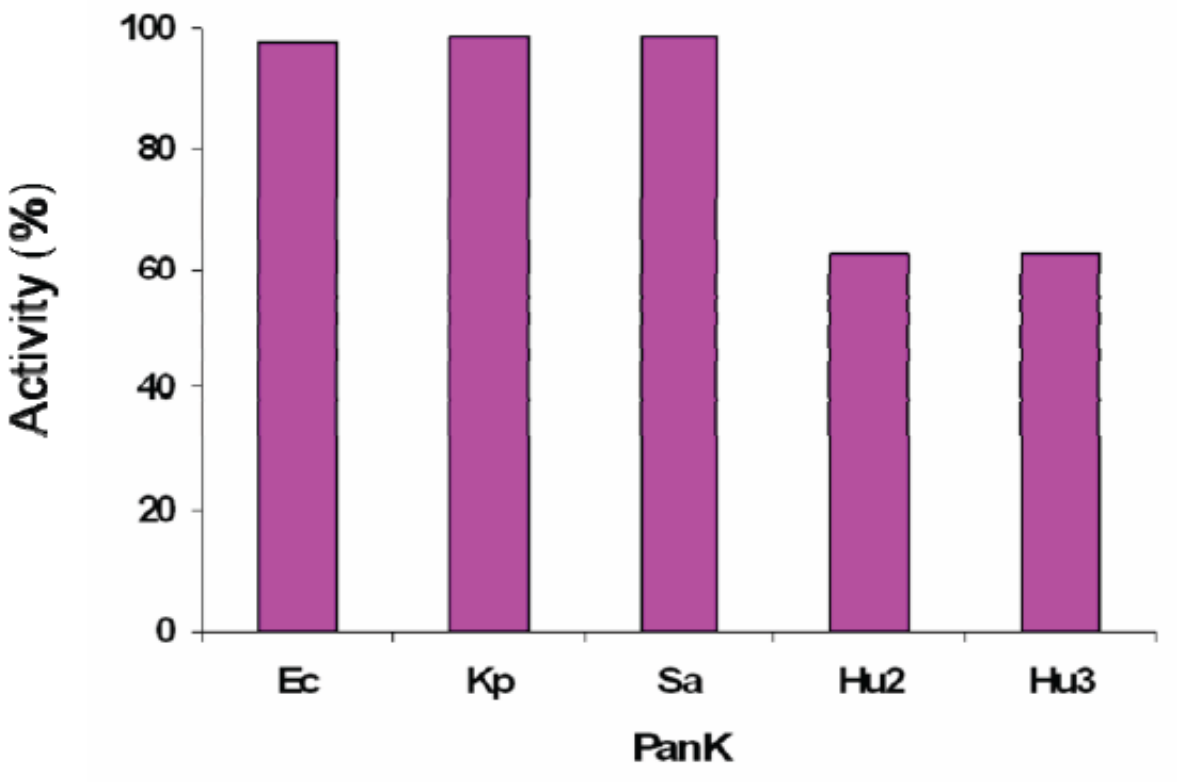

Figure 9. MIC assay of HOPA against *S. aureus*. Bacteria (5x 10^{10} cfu/ml) were grown for one day with increasing concentration of the compound. Data is shown as percent OD_{600} of control.

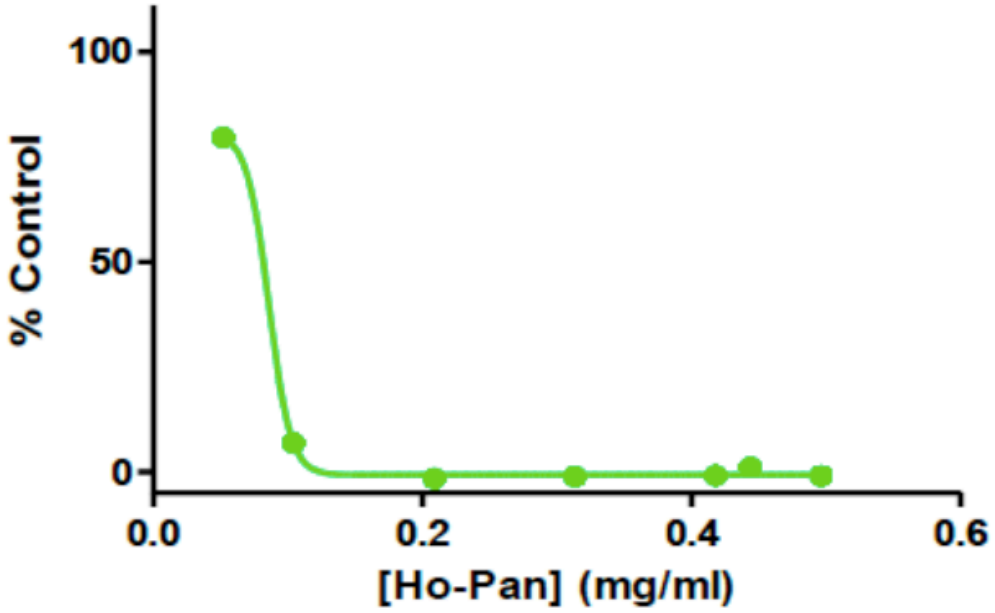

Figure 10. The MT-0190 binding site of SaPanK. *Left,* newly synthesized Pan analogs are shown. *Middle,* MT-0190 (magenta, stick) is bound to both the molecules of SaPank dimer (green and cyan). A zoomed-in view of the MT-0190 binding site shown on the right panel. *Right,* the aromatic moiety of MT-0190 (magenta, carbon) interacts with hydrophobic portions of several residues, L171, T172, E202, V236 and Y240. Dotted line indicates a hydrogen bond between T172 and E202.

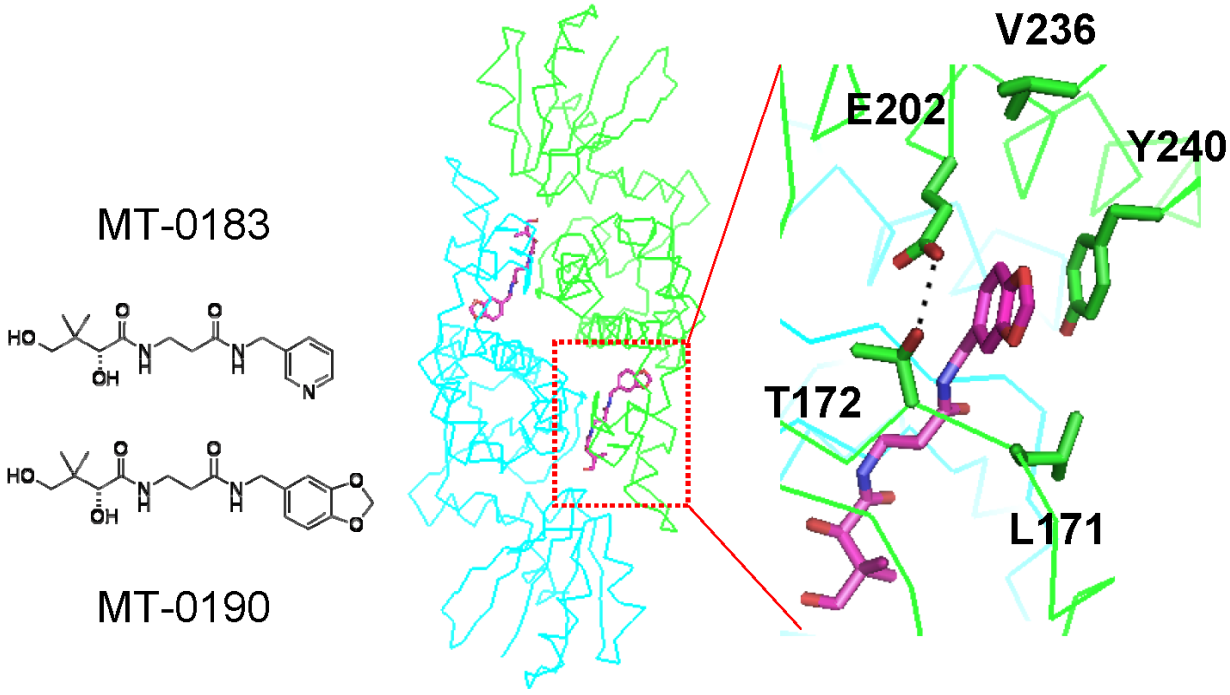

Figure 11. The MT-183 binding pocket of KpPanK. *Left panel,* a view showing the benzyl moiety interactions with hydrophobic residues of KpPanK (Y180, F244, Y258, F259 and Y262). Dotted circle indicates the benzyl moiety. *Right panel,* a view with a horizontal rotation of 90 degrees from the left panel. Dotted circle indicates the same benzyl moiety as in the left panel whereas dotted rectangle shows an alternative binding conformation of the benzyl moiety supported by electron density (data not shown).

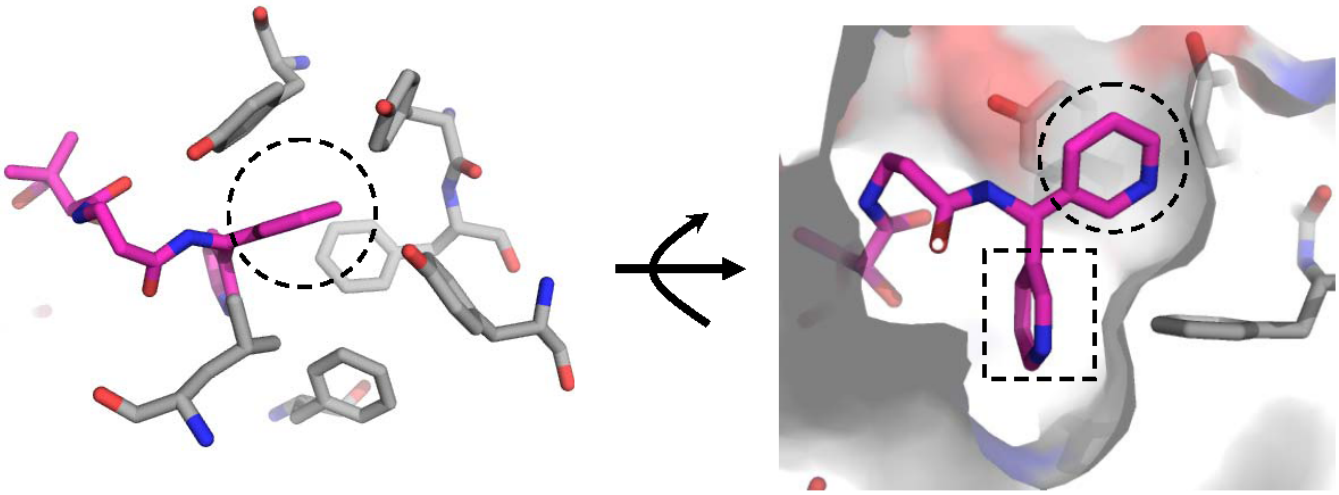

Figure 12. Interactions of N354-Pan with SaPanK and KpPanK.
Left, the kinked conformation of N354-Pan (carbon, purple) interacting with multiple residues of KpPanK (carbon, cyan).

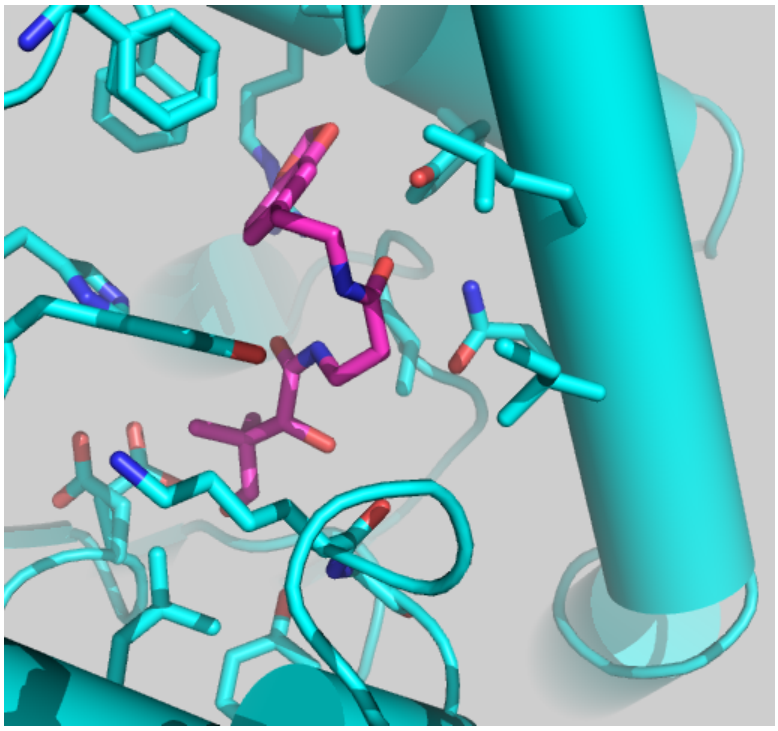

Right, the extended conformation of N354 (carbon, purple) interacting with multiple residue of SaPanK (carbon, grey and yellow). Please notice that the N354-binding pocket is enclosed in one subunit of KpPanK dimer whereas it is formed by both the subunits of SaPanK dimer.